Heliyon 10 (2024) e26845

Contents lists available at ScienceDirect

Heliyon

journal homepage: www.cell.com/heliyon

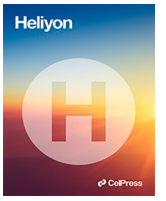

Research article

Optimal placement and operation of soft open points, capacitors, and renewable distributed generators in distribution power networks to reduce total one-year energy loss

Hai Van Tran [a,b], Anh Viet Truong [a], Tan Minh Phan [c], Thang Trung Nguyen [c,*]

[a] Faculty of Electrical and Electronics Engineering, Ho Chi Minh City University of Technology and Education, Ho Chi Minh City, 700000, Vietnam
[b] Faculty of Electrical and Electronics Engineering, Ho Chi Minh City University of Industry and Trade, Ho Chi Minh City, 700000, Vietnam
[c] Power System Optimization Research Group, Faculty of Electrical and Electronics Engineering, Ton Duc Thang University, Ho Chi Minh City, 700000, Vietnam

ARTICLE INFO

Keywords:
Soft open points
Shunt capacitor banks
Distributed generators
Solar radiation
Wind speed

ABSTRACT

The paper optimizes the placement of soft open points (SOPs) devices, shunt capacitor banks (SCBs), and distributed generators (DGs) in the IEEE 69-node distribution power grid for reducing the power loss of a single hour and total energy losses of one year. EO is proven to be more effective than previous methods and three other applied algorithms, including the Coot optimization algorithm (COOT), Modified weight inertia factor and modified acceleration coefficients-based particle swarm optimization (CFPSO), and Tunicate swarm algorithm (TSA). So, EO is applied for the last case considering one SOPs, one wind turbine (WT), two solar photovoltaic systems (PVs), and two SCBs over one year with twelve months and 24 h each month. The study reaches the smallest power loss compared to previous studies in the first case with one SOPs device. The results from the second to the fourth cases indicate that the power grid needs the placement of SCBs and DGs first and SOPs devices to reach the lowest power loss. Case 5 indicates that the hybrid system with one WT and two PVs suffers higher power losses than the base system at hours with high generation from renewable sources; however, integrating the SOPs and SCBs into the hybrid system can reach smaller losses than the base system at these hours. Thus, using SOPs and SCBs in integrated distribution power grids with renewable energies can greatly benefit energy loss reduction.

1. Introduction

Distribution power networks (DPNs) are significant parts of a power system to distribute electricity to electrical loads. As reported, the total power losses in DPNs could equal 13% of the total generated power [1], and high voltage drops at peak hours with a high-power demand of loads were serious [2]. To avoid high power losses and voltage drops, the solution is to reduce the line's operating current and resistance [3] by placing capacitors [4], distributed generators (DGs) [5], WDGs [6], SDGs [7], and DGs based on biomass energy (BMDGs) [8], implementing network reconfiguration (NR) [9], SOPs devices [10], and so on. In the study, the placement of electric components, such as capacitors, soft open points (SOPs), distributed generators based on wind energy (WDGs)

* Corresponding author.
E-mail addresses: haitv.ncs@hcmute.edu.vn (H. Van Tran), anhtv@hcmute.edu.vn (A.V. Truong), phanminhtan@tdtu.edu.vn (T.M. Phan), nguyentrungthang@tdtu.edu.vn (T.T. Nguyen).

https://doi.org/10.1016/j.heliyon.2024.e26845
Received 16 January 2024; Accepted 20 February 2024
Available online 25 February 2024

Nomenclature

N_{dl}	Number of distribution lines
R_{dl}	Resistance of the *dlth* distribution line
$I_{dl,hr,s}$	Operating current of the *dlth* distribution line at the *hrth* hour in the *sth* month
I_{dl}^{max}	Maximum capacity of the *dlth* distribution line
$V_{i,hr,s}$	Voltage at the *i*th node at the *hrth* hour in the *sth* month
V^{min}, V^{max}	Lower and upper limit of node voltage in distribution networks
N_n	Number of nodes in distribution network
N_{SU}, N_{WU}	Number of solar radiation and wind speed-based generating units
$P_{SUm,,hr,s}$	Active power generated by the *mth* solar radiation based generating unit at the *hrth* hour in the *sth* month
$P_{WUk,,hr,s}$	Active power generated by the *kth* wind speed-based generating unit at the *hrth* hour in the *sth* month
$P_{cps,hr,s}$	Active power supplied by the conventional power source at the *hrth* hour in the *sth* month
$P_{Lj,hr,s}, Q_{Lj,hr,s}$	Active and reactive power consumed by the load at the *jth* node at the *hrth* hour in the *sth* month
X_{dl}	Reactance of the *dlth* distribution line
N_{Cap}	Number of capacitor units
$Q_{Cf,hr,s}$	Reactive power generated by the *fth* capacitor unit at the *hrth* hour in the *sth* month
E_m	The solution *m* of the population
RND, γ	Random numbers between zero and one
E_m^{lst}, E_m^{hst}	The lowest and highest limits of the solution *m*
N_{Po}	Population dimension
E_m^{new}	The new *mth* solution
CI, MI	The current iteration index and the maximum iteration index
CP	Scaling factor
ε_1, ε_2	Random numbers between zero and one

and distributed generators based on solar radiation (SDGs), are considered to reach the economic and technical benefits for DPNs.

Basically, the installed DGs can supply active and reactive power to reduce the injection of conventional power sources, meanwhile the SOPs device can change power flows on lines [11]. Both DGs and SOPs can reduce currents on many lines, resulting in the significant loss reduction. The studies [12,13] have investigated the effectiveness of SOPs in DPNs without other active and reactive power sources. Other studies have combined the SOPs devices and other power sources, such as Capacitors [14], DGs [15–17], DGs and NR [18–23], SDGs [24–30], WDGs [31], and both SDGs and WDGs [32–40]. The two studies [12,13] have proved that energy loss was reduced and the voltage was improved, although the study [12] did not consider voltage as an objective like the study [13]. The study [14] indicated that the use of SOPs and Capacitors could reach the best result as compared to the cases without SOPs or with only SOPs and without Capacitors. The study [15] has increased the penetration level of DGs from 0% to 200%, and the best results, thanks to the installation of SOPs, were a 58.4% loss reduction, 68.3% load balance, and 62.1% voltage improvement compared to the case without SOP. The study [16] also combined the SOPs, different penetration levels of DGs, and different Flexible AC Transmission Systems (FACTS). As a result, the 48% and 79% penetration levels were the most optimal for systems with a 50% and 200% load level. The study [17] optimized the penetration level of DGs and SOPs' active and reactive power flows for one day, and it could reduce energy loss by 10%. The study [18] focused on power loss minimization and load balance index minimization for the IEEE 33-node DPN. It indicated that the placement of SOP was more effective than the implementation of network reconfiguration; however, the combination of SOP placement and network reconfiguration was the most effective. The study [19] wanted to use the highest power penetration of DGs and eliminated the use of conventional power sources by combining SOPs placement and network configuration implementation. The study [20] optimized SOPs placement and reconfiguration for the two systems with 33 and 83 nodes for comparison with previous studies. The study [21] has shown that the combination of network reconfiguration and SOPs placement could reach better voltage stability index, loss, and load balancing index than the base system by 31%, 38%, and 27%, respectively. The study [22] optimized the annual SOPs placement, network reconfiguration, and power loss costs. The results indicated that the combination could reach the lowest annual costs. The study [23] simultaneously optimized SOPs placement and NR, and reached the loss reduction up to 63.3% for a 33-node DPN and 82.1% for a 69-node DPN. The study [24] optimized the placement of SOPs and SDGs for a 69-node DPN. It indicated that different locations of SOP led to different power losses and different numbers of nodes violating voltage limits, although the same capacity was applied for different locations. Two studies [25,26] maximized the penetration level of SDGs in the IEEE 33-nodes considering one working day by using three different SOP devices separately. The study [27] minimized the energy curtailment for one working day with the supply from SDGs in the IEEE 33-node DPN. After installing SOP, the energy curtailment was reduced by 84% compared to the case without SOP. The study [28] minimized the total costs of electric devices, purchases, and SDGs for seven cases in the 33-node and 123-node systems. The results indicated that the optimization operation of electric devices such as SOPs, Capacitors, and SDGs could minimize the total costs. The study [29] applied a battery to store energy for SOPs and SDGs to produce electricity for reaching the minimum costs. The study [30] indicated that different locations of SOPs could satisfy all constraints of the systems, but the effectiveness of loss reduction and voltage enhancement was different. The study [31] considered the

placement of SOPs in the 37-node system with the existing WDGs. The placement of one SOPs device could reduce 24% power loss, while the placement of two SOP could reduce the loss by up to 30%. The study [32] considered the same case as [31] but for a 33-node DPN. The study [33] applied a more extensive unbalanced system with 404 nodes in Canada. The study [34,35] considered the DG's penetration levels and selected the highest level that could reach the best objective. The study [36] minimized the total investment and operating costs of OP, DGs, and Capacitors, considering the maximum penetration of DGs. The study [37] focused on the minimum energy curtailment for WDGs and SDGs at peak hours with high generation and low demand. The study [38] applied a mixed-integer second-order cone programming method for a 33-node DPN, while the study [39] modified the method to reach more effective solutions and enlarge the scale of systems to 123 nodes. The study [40] reduced on the power loss for two systems, 33 and 123-node systems by implementing three network analysis methods. As a result, the best method was determined and decided to be the most suitable for the considered problem.

In general, these previous studies have reached significant contributions to the loss reduction, the consideration of renewable energy penetration levels and voltage improvement for standard IEEE DPNs. However, these studies have neglected the combinations of electric components, real data of wind speed and solar radiation, multi periods from months to years. The shortcomings will be overcome in the paper. An effective metaheuristic algorithm, Equilibrium optimizer (EO) [41], is applied for the optimal placement of electric components such as Capacitors, DGs, and SOPs in the IEEE 69-node distribution system. The actual solar radiation and wind speed data in the world are collected using the solar global website [42] and the wind global website [43]. EO has been successfully applied for optimization problems in electrical engineering, such as optimal power grid reconfiguration and optimal placement of SOPs [44], optimal placement of DGs [45], power grid reconfiguration and optimal placement of DGUs [46], and optimal placement of wind power plants in high-voltage power systems [47]. In addition, three other metaheuristic algorithms, including Coot optimization algorithm (COOT) [48], Modified weight inertia factor and modified acceleration coefficients-based particle swarm optimization (CFPSO) [49], and Tunicate swarm algorithm (TSA) [50], are also applied. Compared to previous studies regarding the optimal placement of electric components, the novelties of the work are as follows.

1) Use SOPs to replace switches, which were employed in DPNs after implementing reconfiguration problem to minimize active power loss. In the DPN reconfiguration problem, the switches were placed to connect two nodes, changing power flows and reducing total loss. However, the switches are not as flexible as SOPs in active power exchange between the two nodes and reactive power injection at each node.
2) Try different study scenarios of optimally installing SOPs, capacitors and DGs in DPNs to select the best case for reducing total power loss. The first scenario optimizes placement of one SOPs. The second scenario optimizes the simultaneous placement of one SOPs, capacitors and DGs. The third scenario optimizes the simultaneous placement of capacitors and DGs. The fourth scenario uses the results of the third scenario to optimize one SOPs device. The simulations indicate that different scenarios have different total power loss values.
3) Use the best scenario above to simulate the optimization operation for one year. The DGs are replaced with solar photovoltaic systems and wind turbines. The solar radiation and the wind speeds are taken from areas in Vietnam by using solar global atlas and wind global atlas; meanwhile, the load variation is considered over four seasons. The last simulation can reflect a real operation for a DPN in one year.
4) Apply high new performance metaheuristic algorithms, including EO and COOT, and a popular modified metaheuristic algorithm, CFPSO for the simulations to reach the most effective scenario and the best solution to reduce the energy loss of one year.

After solving the different cases in DPNs with the placement of electric components by using EO, COOT, TSA and CFPSO, the work has main contributions that are summarized as follows.

1) Find the best SOPs, capacitors, and DGs integration to reduce total power loss. Different assumptions of distribution power networks about the existence of active and reactive supply electric devices are implemented for simulations. The power loss results are evaluated to choose the best integration.
2) Optimally determine operating parameters of the installed SOPs device DPNs with the existence of capacitors and DGs over one year. DGs are solar and wind-based power generating sources in which solar and wind can be collected in an actual area in the world. The optimal energy loss over one year indicates that previous studies considering 1 h or day to allocate SOPs in the distribution system optimally did not reach the best solution.
3) Indicate that the use of high penetration level of renewable energies can suffer higher energy loss than the systems without the renewable energies.

2. Problem formulation

In the study, the generation of capacitors, WDGs and SDGs is considered to reduce the power supplied from the conventional power source at the slack bus and the current on distribution lines. In addition, a SOPs device is also used to transmit active power between two terminals and produce reactive power at each terminal. Thanks to the operation of the electric components, the current, voltage drop, and energy loss on distribution lines can be reduced. So, the study focuses on energy loss reduction and satisfies the operating constraints of the system involving voltage profile. The objective and constraints are expressed as follows.

2.1. Objective function

The total energy loss reduction of one operating year is the major objective, as shown in the following model:

$$\text{Reduce } OE_{loss} = \sum_{s=1}^{N_{ms}} \sum_{dl=1}^{N_{dl}} N_{day,s}.\left(3.I_{dl,hr,s}^{2}.R_{dl}\right) \text{ (kWh)} \tag{1}$$

Where OE_{loss} is the total one-year energy losses; N_{ms} is the number of months in one year, and it is set to twelve. $N_{day,s}$ is the number of days in the *sth* month. It is noted that the first month is January and the second month is February, and the last month is December. All months have a certain day number, excluding February with twenty-eight or twenty-nine days. In this study, twenty-eight is used for February.

2.2. Constraints

Distribution line capacity limit: Each distribution line connects two nodes. Each line is a conductor with a predetermined current limit. The current limit is also called the maximum capacity of the distribution line, and the operating current must be equal to or smaller. The following inequality is the constraint of the distribution line:

$$I_{dl,hr,s} \leq I_{dl}^{max} \tag{2}$$

Load voltage limits: In the distribution power network, the voltage at each node is constrained by a predetermined range between the upper and lower limits for stable operation. The constraint is as follows:

$$V^{min} \leq V_{i,hr,s} \leq V^{max}; i = 1, \ldots, N_n \tag{3}$$

Power balance constraints: The study considers the installation of capacitors, SUs, WUs, and SOPs in distribution networks. Capacitors and SOPs can produce reactive power; meanwhile, SDGUs and WDGUs can supply active power. So, the active and reactive power balance equalities are written as follows:

$$\sum_{m=1}^{N_{SU}} P_{SUm,hr,s} + \sum_{k=1}^{N_{WU}} P_{WUk,hr,s} + P_{cps,hr,s} = \sum_{dl=1}^{N_{dl}} 3.R_{dl}.I_{dl,hr,s}^{2} + \sum_{j=1}^{N_n} P_{Lj,hr,s} \tag{4}$$

$$\sum_{f=1}^{N_{Cap}} Q_{Cf,hr,s} + Q_{cps,hr,s} = \sum_{dl=1}^{N_{dl}} 3.X_{dl}.I_{dl,hr,s}^{2} + \sum_{j=1}^{N_n} Q_{Lj,hr,s} \tag{5}$$

Generation limits of capacitors*, SUs, WUs*: At each hour, the power generation of the added electric components is constrained by the minimum and maximum capacity as the following models:

$$P_{SUm}^{min} \leq P_{SUm,hr,s} \leq P_{SUm}^{max} \tag{6}$$

$$P_{WUk}^{min} \leq P_{WUk,hr,s} \leq P_{WUk}^{max} \tag{7}$$

$$Q_{Cf}^{min} \leq Q_{Cf,hr,s} \leq Q_{Cf}^{max} \tag{8}$$

Where P_{SUm}^{min} and P_{SUm}^{max} are the minimum and maximum generation limit of the *mth* solar radiation-based generating unit; P_{WUk}^{min} and P_{WUk}^{max} are the minimum and maximum generation limit of the *kth* wind speed-based generating unit; Q_{Cf}^{min} and Q_{Cf}^{max} are the minimum and maximum generation limits of the *fth* capacitor unit. In the study, the minimum generation limit of these components is selected to be 0 MW for all SUs and WUs and 0 MAVr for all capacitors; meanwhile, the maximum generation limit is optimally determined by using the maximum load factor at the peak hour. There are different load factors for different hours in seasons, and the highest load factor, 1.0 pu, will be used to optimally find the maximum generation limit of all added electric components.

Location limits of capacitors*, SUs, WUs*: The study only considers pure active power generation for SUs and WUs and pure reactive power generation for capacitors. Capacitors can have the same locations as SUs and WUs, and the overlapped nodes can be injected reactive and active power by either capacitors and SUs or by capacitors and WUs. However, SUs and WUs cannot be placed at the same locations. Basically, these components can be installed in a distribution power network with the location from node 2 to node N_n. So, the inequalities below are applied for the location constraints:

$$2 \leq L_{SUm},\ L_{WUk},\ L_{Cf} \leq N_{node} \tag{9}$$

$$L_{SUm} \neq L_{WUf} \tag{10}$$

Where L_{SUm} and L_{WUk} are the locations the *mth* solar radiation and wind speed-based generating unit; and L_{Cf} is the location of the *fth* capacitor unit.

2.3. Model and constraints of SOPs devices

Model of SOPs: SOPs device is a power electronic device that can control active power flow between adjoining feeders and compensate reactive power through its connecting nodes. This paper considers the SOPs devices as voltage source converters (VSC) with back-to-back connections that can replace ordinarily open switches in distribution power networks. Respectively considering node m and node n as open points on feeder 1 and feeder 2, a general connection of the SOPs device is shown in Fig. 1.

Constraints of SOPs: The related variables of the SOPs device in Fig. 1 are comprised of $P_{VSC,m}$, $P_{VSC,n}$, $Q_{VSC,m}$ and $Q_{VSC,n}$. $P_{VSC,m}$ and $P_{VSC,n}$ are the active power injections at nodes *m* and *n*, respectively. $Q_{VSC,m}$ and $Q_{VSC,n}$ are the reactive power injections at nodes *m* and *n*, respectively. In this work, the power loss of the SOPs is neglected because this loss of a VSC is very low, approximately 1% per converter [51]. The relationship between the SOPs device's parameters can be mathematically expressed by Refs. [18,21]:

$$P_{VSC,m} + P_{VSC,n} = 0 \tag{11}$$

$$S_{VSC,m} = \sqrt{P_{VSC,m}^2 + Q_{VSC,m}^2} \tag{12}$$

$$S_{VSC,n} = \sqrt{P_{VSC,n}^2 + Q_{VSC,n}^2} \tag{13}$$

$$0 \le S_{VSC,m}, S_{VSC,n} \le S_{SOPs} \tag{14}$$

Where $S_{VSC,m}$ and $S_{VSC,n}$ are the operating apparent power of the SOPs device at nodes *m* and *n*, respectively. S_{SOPs} is the rated apparent power of the SOPs device. There are two cases for parameters in Equation (11): 1) $P_{VSC,m} < 0$ and $P_{VSC,n} > 0$ means the power is moved from node *m* to node *n*, and 2) $P_{VSC,n} < 0$ and $P_{VSC,m} > 0$ means the power is moved from node *n* to node *m*.

3. Equilibrium Optimizer.

In the optimization process, EO also utilizes a particular population at the beginning, and each population element is considered a feasible solution to the given problem. EO's structure consists of the following main steps.

2.4. The initialization

In the first step, EO requires a random solution set to start its optimization process. The initial set is produced based on the lowest and highest limit of the solutions as follows:

$$E_m = E_m^{lst} + RND \times \left(E_m^{hst} - E_m^{lst}\right) \; with \; m = 1, \ldots, N_{Po} \tag{15}$$

2.5. The solution update procedure

After the initialization is completed, the update procedure for new solutions is executed. The update procedure improves the quality of the current solutions after each iteration. The mathematical expression for finding a new solution is as follows:

$$E_m^{new} = E_{ref} + \left(E_m - E_{ref}\right) \times EM + \frac{GP}{RP \times V} \times (1 - EM) \tag{16}$$

In the equation, *RP* is the return proportion in the given volume (*V*) and it is calculated by the fraction of rated flow (*RF*) through the model and *V*. E_{ref}, *EM*, and *GP* are, respectively, the reference solution, the exponential multiplier, and the generating proportion. The three factors are calculated as follows:

The determination of E_{ref}: E_{ref} is one out of five elements as presented in Equation (17). Among the five elements, E_{MB} is a center solution obtained by using Equation (18), meanwhile four others, including E_{ref1}, E_{ref2}, E_{ref3} and E_{ref4} are the four leading solutions with the smallest fitness function values in the current population. Here, we are considering EO for minimization optimization problems.

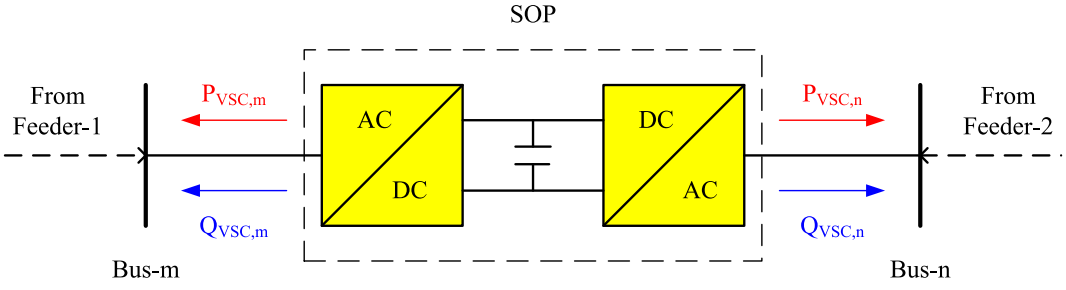

Fig. 1. Single SOP connected bus-m and bus-n in DN.

$$E_{ref} \in \left[E_{ref1}, E_{ref2,} E_{ref3}, E_{ref4}, E_{MB}\right] \tag{17}$$

$$E_{MB} = \frac{E_{ref1} + E_{ref2} + E_{ref3} + E_{ref4}}{4} \tag{18}$$

The calculation of EM: In metaheuristic algorithms, *EM* is regarded as a scaling factor to produce jumping steps between old and new solutions. Normally, the factor is a random value in a determined range. However, this factor significantly balances the exploration and exploitation during the optimization process in EO. The factor is a function obtained by:

$$EM = 2 \times sign(\gamma - 0.5) \times [e^{-tv} - 1] \tag{19}$$

where *tv* is the time variation factor obtained by:

$$tv = \left(1 - \frac{CI}{MI}\right)^{\frac{CI}{MI}} \tag{20}$$

The calculation of GP: GP is another implementation to enhance more balance between the exploration and the exploitation abilities in the optimization process besides EM.

$$GP = EM \times CP\left(E_{ref} - tv \times E_m\right) \tag{21}$$

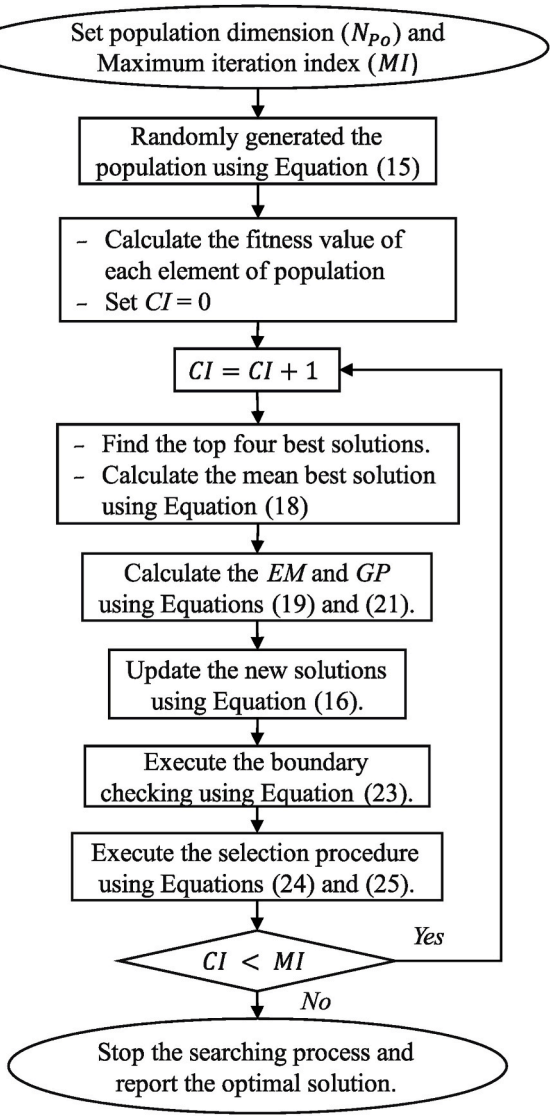

Fig. 2. Using EO for solving a general optimization problem.

Where,

$$CP = \begin{cases} \frac{\varepsilon_1}{2}, if\ \varepsilon_2 \geq 0.5 \\ 0, \text{otherwise} \end{cases} \tag{22}$$

2.6. The correction of new solutions

After finding new solutions obtained by using Equation (16), the limitations of solutions are used to check and correct the new ones as follows:

$$E_m^{new} = \begin{cases} E_m^{lst} \text{ if } E_m^{new} < E_m^{lst} \\ E_m^{hst} \text{ if } E_m^{new} > E_m^{hst} \\ E_m^{new}, \text{otherwise} \end{cases} \tag{23}$$

2.7. The selection procedure

The main purpose of implementing this step is to save the high-quality solutions for the next iteration and abandon the poor-quality ones. The selection procedure is executed based on the comparison of the fitness values belonging to the old solutions and the new ones, as presented by:

$$Ft_m = \begin{cases} Ft_m^{new} \text{ if } Ft_m \geq Ft_m^{new} \\ Ft_m, \text{otherwise} \end{cases} \tag{24}$$

And

$$E_m = \begin{cases} E_m^{new} \text{ if } Ft_m \geq Ft_m^{new} \\ E_m, \text{otherwise} \end{cases} \tag{25}$$

In Equations (24) and (25), Ft_m and Ft_m^{new} are, respectively, the current and new fitness values of the solution m.

2.8. EO' iterative algorithm

The whole optimization process of EO is described in Fig. 2.

3. Simulation results

In this section, four meta-heuristic algorithms, consisting of CFPSO, COOT, TSA, and EO, are implemented to solve the optimal placement of electric components in two DPNs. Two study cases are simulated in the first system, and five are simulated in the second.

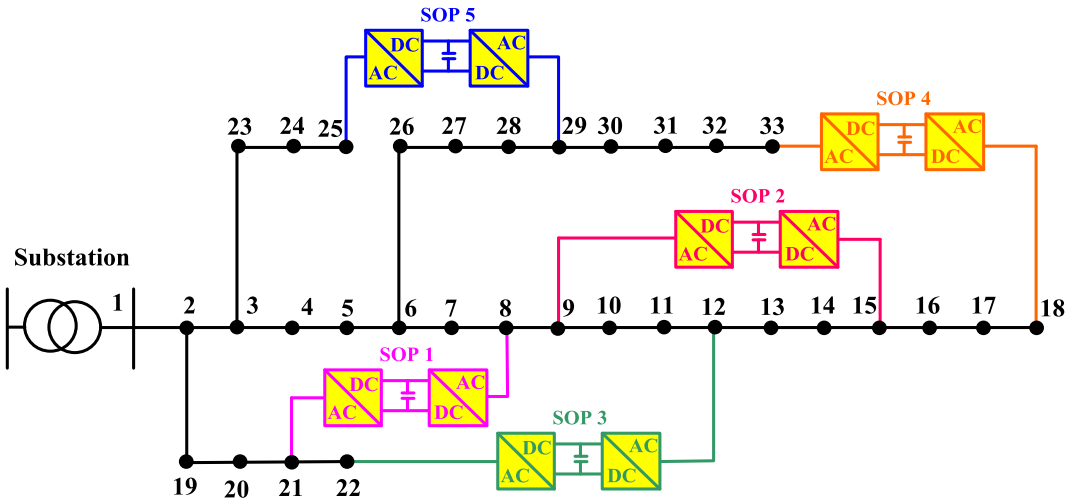

Fig. 3. The modified IEEE 33-node system with five availableavailable SOPs devices.

Each method is run 50 times on a computer with 8.0-GB RAM and the 1.8-GHz processor in Matlab program language for each study case. The population and iteration numbers are set to 20 and 100 for the first system and 20 and 150 for the second system.

3.1. Study cases in the IEEE 33-node DPN

The section shows two study cases in the IEEE 33-node DPN: Case 1) Optimal placement of three DGs and Case 2) Optimal placement of three DGs and five SOPs devices. The IEEE 33-node DPN's configuration with the five available SOPs devices is presented in Fig. 3. The system's data are shown in Ref. [52] and Table A1 in Appendix. The five SOPs devices are located between nodes 8–21, 9–15, 12–22, 18–33, and 25–29 [53]. The nominal voltage of the system is 12.66 kV voltage. The load demand is 3.715 MW for active power and 2.3 MVAr for reactive power. The active power loss of the original system without SOPs and DGs is 210 kW [52,53]. The lower and upper voltage limits for all the buses were fixed to 0.95 pu. And 1.05 pu. The minimum and maximum limits of the SOPs are 0 MVA and 3 MVA; meanwhile, the limits of DGs are 0–2 MW. The results from EO were compared to those from COOT, CFPSO, TSA, TM (Taguchi Method) [54], MOTA (Multi-objective taguchi approach) [54], BA (Bat algorithm) [55], and HSA (Harmony search algorithm) [56].

3.1.1. *Case 1*: Optimal placement of three DGs

Table 1 compares the location and capacity of three DGs, power loss, and loss reduction compared to the base system. The solution from EO has reached the power loss of 72.7869 kW, which is as good as that from COOT and TSA but smaller than that of the other remaining algorithms. Compared to the base system, EO, COOT, and TSA can reach a 65.34% power loss reduction, while that of others is from 49.52% to 65.30%. EO and COOT have selected nodes 13, 24, and 30 with a total capacity of 2946.67 kW. CFPSO, TSA, and PSO [53] also selected the same nodes as EO but used different capacities. Other algorithms have selected different nodes and different capacities. The EO solution is feasible and high in quality. So, EO is more effective than these algorithms in Refs. [53–56] and CFPSO when placing three DGs in the system.

3.1.2. *Case 2*: Optimal placement of three DGs and five SOPs devices

Table 2 compares the results obtained by EO, COOT, CFPSO, TSA, and PSO [53]. The locations of five SOPs devices were predetermined at lines 8–22, 9–15, 12–22, 18–33, and 25–29 [53]. In contrast, the applied algorithms determined other parameters, such as the operating parameters of SOPs devices and the location and capacity of DGs. The study [53] did not report the operating parameters of the five SOPs devices, and these parameters found by EO, TSA, COOT, and CFPSO were not the same. All applied algorithms and PSO [53] found different solutions to the location and capacity of DGs. As a result, EO reached the smallest power loss of 5.6916 kW, but that of others was from 5.8301 kW to 43.167 kW. EO reaches a 97.29% loss reduction compared to the base system, while others reach 79.5%–97.22%. EO is more effective than COOT, TSA, CFPSO, and PSO [53] for the study case.

Fig. 4 presents the voltage profiles of cases, where those of Cases 1 and 2 are derived from EO's optimal solutions. Many nodes in the base case violated the lower voltage bound once their voltage was under 0.95 pu. On the contrary, Cases 1 and 2 improved the voltage, especially Case 2, with an approximate voltage of 1.0 pu for all nodes. The indication shows the significant contribution of integrating DGs and SOPs devices in the IEEE 33-node system.

3.2. Study cases in the IEEE 69-node DPN

The section investigates the optimal placement of SOPs devices, DGs, and capacitors in a modified IEEE 69-node system. The system's single-line configuration is shown in Fig. 5, and its data is reported in Table A2 in Appendix [57]. The total power loss of all lines in the base system without electric components is 225.01 kW [13,15]. In the modified system, we consider eight more lines, called L1, L2, L3, L4, L5, L6, L7, and L8. The study [15] has implemented network reconfiguration and used switches to connect nodes: Lines L1, L2, L3, L4, and L5. Then, the study continued to optimize the placement of one SOPs device, and L4 was the most suitable line. On the other hand, the study [13] has proposed using L6, L7, and L8 for placing SOPs devices. In this study, we combine the two studies [13,15] to modify the IEEE 69-node system, and we perform the five following study cases as follows.

Case 1. Employ the modified IEEE 69-node DPN in Fig. 5 to optimize the operating parameters of one SOPs device at eight different

Table 1
Comparison of power loss for the IEEE 33-node DPN with three DGs.

Algorithm	Total DG Size (kW)	Connected buses	Power loss (kW)	Loss reduction (%)
PSO [53]	3040.00	13; 30; 24	72.85	65.30
TM [54]	2879.50	15; 33; 26	102.3	49.52
MOTA [54]	3280.00	7, 30, 14	96.3	52.48
BA [55]	2721.00	15, 30, 25	75.05	64.42
HSA [56]	1725.60	18, 33, 17	96.76	52.26
EO	2946.67 (1091.33; 801.7; 1053.64)	24; 13; 30	72.7869	65.34
COOT	2946.67 (1091.33; 801.7; 1053.64)	24; 13; 30	72.7869	65.34
CFPSO	2949.63 (803.98; 1092.22; 1053.43)	13; 24; 30	72.7871	65.34
TSA	2946.72 (801.77; 1053.34; 1091.61)	13; 30; 24	72.7869	65.34

Table 2
Results obtained for the IEEE 33-node DPN with three DGs and five SOPs devices.

Algorithm	DGs' Location-Size (kW)	SOPs devices' operating power (MVA)	Power Loss (kW)-Loss reduction (%)
EO	32–660.8061; 8–1167.532; 29–1311.5086	$S_{VSC,8} = 0.55$; $S_{VSC,21} = 0.51$; $S_{VSC,9} = 0.18$; $S_{VSC,15} = 0.21$; $S_{VSC,12} = 0.24$; $S_{VSC,22} = 0.22$; $S_{VSC,18} = 0.22$; $S_{VSC,33} = 0.38$; $S_{VSC,25} = 0.89$; $S_{VSC,29} = 1.04$	5.6916–97.29
COOT	21–1126.6312; 25–1320.0238; 18–666.4594	$S_{VSC,8} = 0.67$; $S_{VSC,21} = 0.64$; $S_{VSC,9} = 0.16$; $S_{VSC,15} = 0.19$; $S_{VSC,12} = 0.22$; $S_{VSC,22} = 0.21$; $S_{VSC,18} = 0.43$; $S_{VSC,33} = 0.52$; $S_{VSC,25} = 0.66$; $S_{VSC,29} = 0.86$	5.8301–97.22
CFPSO	19–992.8255; 2–1947.4126; 3–2000	$S_{VSC,8} = 1.07$; $S_{VSC,21} = 1.02$; $S_{VSC,9} = 2.79$; $S_{VSC,15} = 2.75$; $S_{VSC,12} = 2.4$; $S_{VSC,22} = 1.23$; $S_{VSC,18} = 1.63$; $S_{VSC,33} = 1.94$; $S_{VSC,25} = 1.63$; $S_{VSC,29} = 0.82$;	5.9810–97.15
TSA	14–884.866; 25–1010.8302; 30–1010.5999	$S_{VSC,8} = 0.23$; $S_{VSC,21} = 0.27$; $S_{VSC,9} = 0.2$; $S_{VSC,15} = 0.2$; $S_{VSC,12} = 0.21$; $S_{VSC,22} = 0.23$; $S_{VSC,18} = 0.2$; $S_{VSC,33} = 0.55$; $S_{VSC,25} = 0.06$; $S_{VSC,29} = 0.09$	19.8218–90.56
PSO [53]	8-NR; 24-NR; 32-NR	–	43.167–79.5

NR: Not reported.

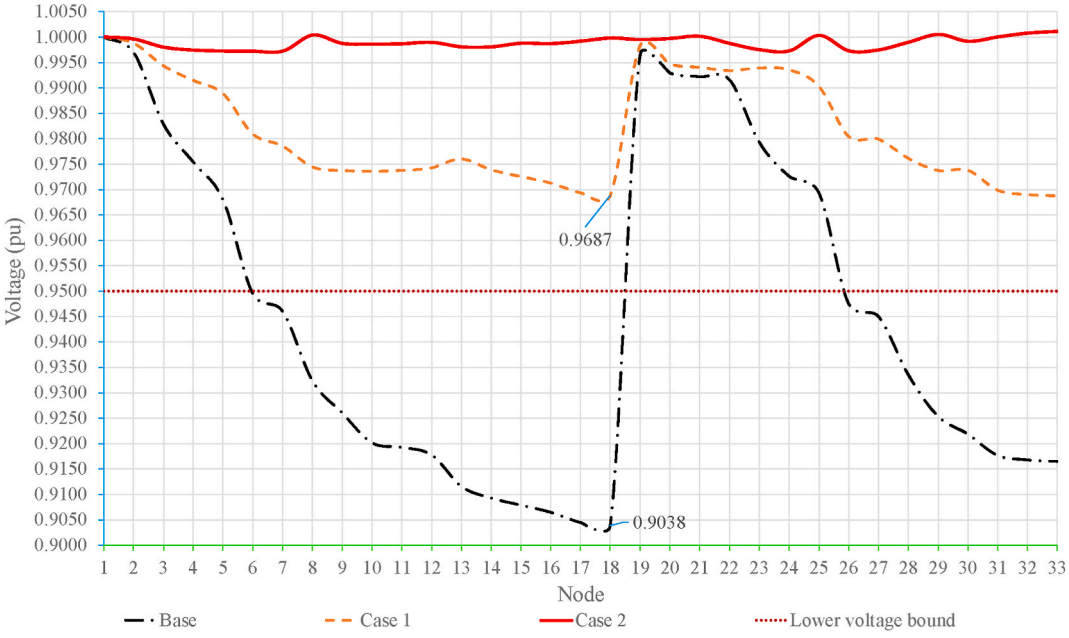

Fig. 4. Voltage profiles of the IEEE 33-node DPN.

lines.

Case 2. Optimize the simultaneous placement of one SOPs device, capacitors, and DGs.

Case 3. Optimize the simultaneous placement of capacitors and DGs.

Case 4. Use the determined capacitors and DGs in Case 3 to optimize one SOPs device.

Case 5. Optimally operate the placed SOPs device over one day with actual data of solar radiation and wind speed.

3.2.1. 4.2.1. Case 1: optimize operating parameters of one SOPs device

In Case 1, EO, CFPSO, TSA and COOT are employed to find the optimal operating parameters of one SOPs device, which is placed on

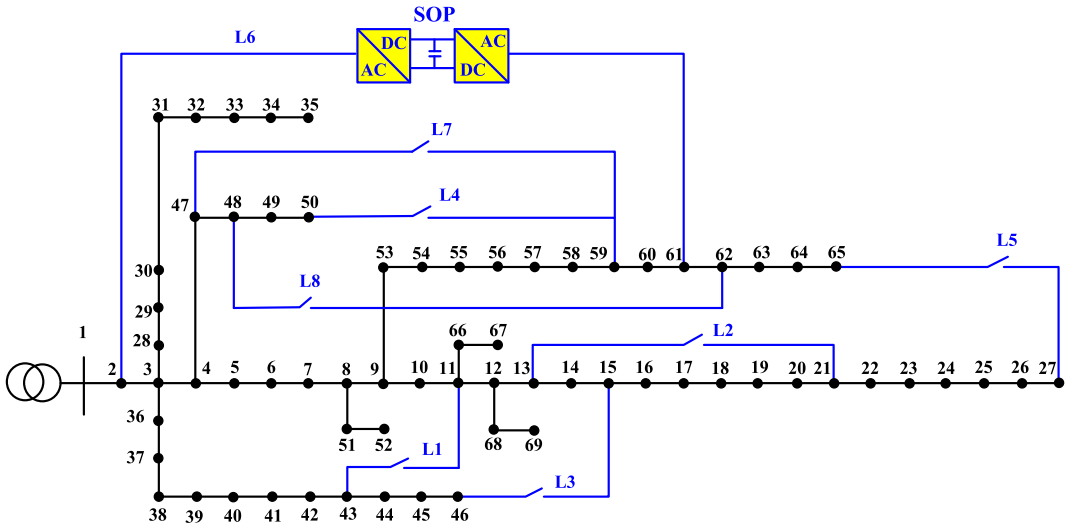

Fig. 5. The modified IEEE 69-node RPN.

each of the lines L1 to L8. The capacity of the SOPs device is selected to be 3.0 MVA [27]. The best and worst power losses from the fifty runs are reported in Table 3. EO can reach the same minimum losses as COOT and TSA but better minimum losses than CFPSO for different locations of the SOPs. However, EO can reach better maximum losses than COOT, TSA and CFPSO. So, EO is significantly superior to CFPSO, TSA and COOT. Looking through the minimum losses of EO can see that the placement of the SOPs device on Line L6 can reach the best minimum loss of 23.2 kW; meanwhile, the worst minimum loss of 206.26 kW is the result of placing the SOPs on Line L2. Line L6 connects node 2 and node 61. Line 2 connects node 13 and node 21. The placement of the SOPs device on other lines leads to the second-best minimum loss of 28.50 kW and the second-worst minimum loss of 189.01 kW.

Table 4 presents the active power flows and reactive injections at each of the SOPs terminals together with the result of power loss. We focus on the best loss of 23.2 kW corresponding to Line L6, the middle loss of 59.821 kW corresponding to Line L4, and the worst loss of 206.26 kW corresponding to Line L2. The SOPs on Line L6 moved the active power of 1.83 MW from node 2 to node 61; meanwhile, it produced reactive power of 1.47 MVAR and 1.3 MVAR at nodes 2 and 61. The SOPs on Line L2 moved a small active power of 0.298 MW from node 13 to node 21, and it also produced a small reactive power of 0.586 MVAR at node 13 and 0.199 MVAR at node 21. The SOPs on Line 4 moved the active power of 1.6775 MW from node 50 to node 59, producing the reactive power of 0.5538 MVAR and 1.3527 MVAR at nodes 50 and 59, respectively. The active power moved between two nodes and the reactive power generated at the nodes are relatively high to cut the line current, leading to loss reduction. Compared to the SOPs on Line L6, the SOPs on Line L7 moved a higher active power of 1.9191 MW but generated a lower reactive power of 0.9295 MVAR. However, the power loss of the SOPs on Line L7 suffers a higher loss of 20.61 kW than on L6, equal to 88.8% of the loss from the SOPs on L6.

By referring to Equations (11)–(13), we can check the operating constraints of the SOPs device on Line L6. The SOPs took the active power of 1.83 MW at node 2 (i.e., $P_{VSC,2} = -1.83$ MW) and transmitted the power to node 61 (i.e., $P_{VSC,61} = 1.83$ MW). So, the constraint (11), which is $P_{VSC,2} + P_{VSC,61} = -1.83 + 1.83 = 0$, is satisfied exactly. On the other hand, the SOPs injected the reactive power at nodes 2 and 61 (i.e., $Q_{VSC,2} = 1.47$MVAR and $Q_{VSC,61} = 1.3$ MVAR). Based on Equations (12) and (13), we obtain $S_{VSC,2} = 2.35$ (MVA) and $S_{VSC,2} = 2.24$ (MVA). Recall that the capacity of the SOPs device is 3 MVA; thus, the operating apparent values, 2.35 and 2.24 MVA, are smaller than the rated apparent of the SOPs.

The computational efficiency of EO is compared with Modified Particle Swarm Optimization (MPSO) [13], Cuckoo search algorithm (CSA) [13], Aquila Optimizer (AO) [13], differential squirrel search algorithm (DSSA) [13], and local search technique-based Particle Swarm Optimization (LSPSO) [15], as shown in Table 5. Regarding the contribution to loss reduction, the proposed

Table 3
The minimum and maximum power losses for different locations of the SOPs device.

SOPs' Location	The minimum power loss (kW)				The maximum power loss (kW)			
	EO	CFPSO	COOT	TSA	EO	CFPSO	COOT	TSA
L1	181.00	181.01	181.00	181.00	181.00	181.44	181.01	186.24
L2	206.26	206.29	206.26	206.27	206.26	208.72	206.28	208.53
L3	189.01	189.03	189.01	189.01	189.01	211.58	189.01	192.22
L4	59.82	59.84	59.82	59.83	59.82	60.51	59.83	74.49
L5	147.16	147.20	147.16	147.16	147.16	163.85	147.18	163.36
L6	23.20	23.21	23.20	23.20	23.20	23.41	23.21	24.85
L7	43.81	43.82	43.81	43.81	43.81	44.22	43.82	48.72
L8	28.50	28.51	28.50	28.51	28.50	29.07	28.50	36.50

Table 4
Operating parameters of the SOPs device on different lines.

Line	From node m	To node n	$P_{VSC,m}$ (MW)	$Q_{VSC,m}$ (MVAr)	$P_{VSC,n}$ (MW)	$Q_{VSC,n}$ (MVAr)	Power loss (kW)
L1	43	11	−1.0612	0.0788	1.0612	1.2461	181
L2	13	21	−0.298	0.586	0.298	0.199	206.26
L3	46	15	−0.688	0.071	0.688	0.589	189.01
L4	50	59	−1.6775	0.5538	1.6775	1.3527	59.82
L5	27	65	−0.366	0.300	0.366	0.950	147.16
L6	2	61	−1.83	1.47	1.83	1.30	23.2
L7	47	59	−1.9191	0.9295	1.9191	1.3538	43.81
L8	48	62	−1.7622	0.6442	1.7622	1.2825	28.5

Table 5
The best placement of different algorithms for Case 1.

Method	The selected line	Power loss (kW)	Loss reduction (kW)	Loss reduction (%)
Ref. [15]	–	225	–	–
LSPSO [15]	L4	60.00	165.00	73.33
MPSO [13]	L7	63.39	161.61	71.83
CSA [13]	L8	57.16	167.84	74.60
DSSA [13]	L6	42.60	182.40	81.07
AO [13]	L6	42.59	182.41	81.07
EO	L6	23.2	201.80	89.69

solution of EO can significantly reduce the loss from 225 kW to 23.1956 kW; meanwhile, the second-best algorithm, AO [13], and the worst algorithm MPSO [13] reduce the loss to 42.59 and 63.39 kW. Compared to the loss of the base system, EO can reach a lower loss by 201.8 kW, equivalent to 89.69% of the initial loss. Similarly, the second-best and worst algorithms, AO and MPSO in Ref. [13], reach lower losses by 182.41 and 161.61 kW, respectively. The loss reduction in % from AO and MPSO is 71.83% and 81.07%, respectively. Thus, EO is more suitable than others for solving the placement of SOPs devices in the IEEE 69-node RPD.

Concerning the selected line to place the SOPs device can indicate that Line L6 connecting node 2 and node 61 is more optimal than other lines, such as Lines L4, L7, and L8, which were selected by LSPSO [15], MPSO [13] and CSA [13]. The top three algorithms, including DSSA [13], AO [13], and EO selected the same Line L6; However, EO is more optimal than DSSA and AO in finding the operating parameters, active and reactive powers. To clarify the outstanding performance of EO over DSSA and AO [13], Table 6 is formed. EO, DSSA, and AO moved 1.83, 1.37, and 1.38 MW from node 2 to node 61, respectively. Furthermore, the operating apparent of EO, DSSA, and AO is 2.35, 2.84, and 2.84 MVA. EO moved a greater active power than DSSA and AO, but EO's operating apparent is smaller than DSSA's and AO's. The highest apparent power of EO is 2.35 MVA, but that is 2.84 MVA for DSSA and AO.

The power loss on each branch in the base and hybrid system without and with the SOPs is plotted in Fig. 6. The branch loss in the hybrid system is equal to or smaller than in the base system. Especially on Branches 2–8 and 51–60, the loss in the hybrid system is much smaller than the base system. The high difference is why the total loss in the base system is very high, 225 kW, while that in the modified system is much smaller, only 23.2 kW.

Fig. 7 shows the SOPs'location's impact on the hybrid system's voltage profile. In the simulation of results, the minimum and maximum voltage limits were applied to be 0.9 and 1.0 Pu. So, the figure indicates that all cases can satisfy the voltage constraints. However, a voltage close to 1.0 Pu is still the best. We have drawn two voltage curves of 0.95 Pu and 1.0 Pu. The base system and the hybrid system with the SOPs on Line 2 and Line 3 had smaller voltage values than 0.95 Pu at the same nodes, 57–65.

Similarly, the hybrid systems with the SOPs device on Lines L1 and L5 had smaller voltage values than 0.95 at nodes 58–65 and 59–65. In addition, the hybrid system with SOPs on Line L5 had nodes 23–27 with a lower voltage than 0.95 Pu. However, other remaining hybrid systems with SOPs devices on Lines 4, 6, 7, and 8 could reach better profiles. Using Equation (2) in the study [58] to calculate the total voltage deviation (TVD), Table 7 is established to rank the voltage profile improvement of different cases, from the base system to the eight hybrid systems with SOPs at Lines L1-L8. The hybrid system with SOPs on Line L6 (HS-L6) can reach the best voltage profile with the smallest TVD, 0.587 Pu. The cases with the second-best and the worst voltage profiles are the hybrid system with the SOPs on L8 and the base system without SOPs. In summary, the hybrid system with the placement of the SOPs device on Line L6 could reach the lowest power loss and the best voltage profile.

Table 6
Comparison of EO performance with DSSA and AO.

Algorithm	$P_{VSC,61}$ (MW)	$Q_{VSC,61}$ (MVAr)	$S_{VSC,61}$ (MVA)	$P_{VSC,2}$ (MW)	$Q_{VSC,2}$ (MVAr)	$S_{VSC,2}$ (MVA)	Loss (kW)	Loss reduction
DSSA [13]	1.37	0.71	1.55	−1.37	2.48	2.84	42.60	81.06%
AO [13]	1.38	0.71	1.55	−1.38	2.48	2.84	42.59	81.07%
EO	1.83	1.30	2.24	−1.83	1.47	2.35	23.196	89.69%

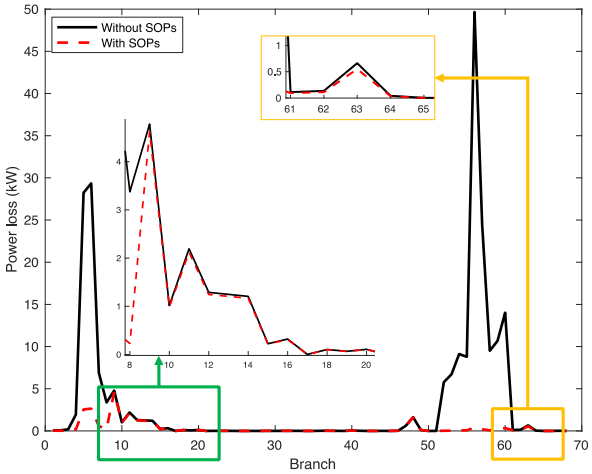

Fig. 6. Power loss on distribution lines in IEEE 69-bus radial distribution system before and after placing SOP.

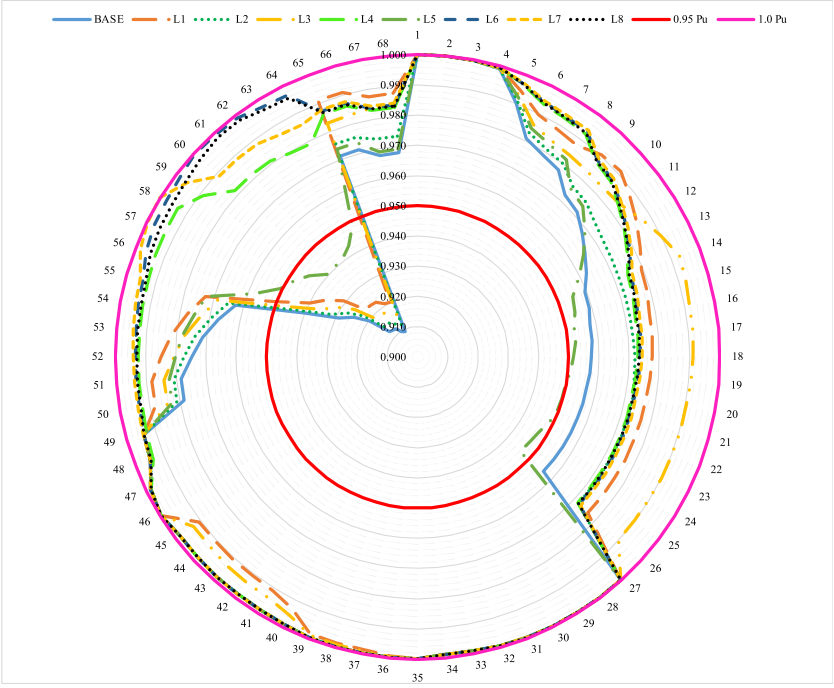

Fig. 7. Voltage profiles in DN before and after placing SOP.

Table 7
Voltage deviation index and rank of voltage profile in different cases.

System	TVD	Rank of TVD
Base	1837	9
HS-L1	1255	6
HS-L2	1549	7
HS-L3	1177	5
HS-L4	0,730	4
HS-L5	1616	8
HS-L6	0,587	1
HS-L7	0,619	3
HS-L8	0,618	2

3.2.2. Cases 2-4: Optimize the placement of SOPs, capacitors and DGs

This section investigates the effectiveness of applying SOPs, capacitors, and DGs by implementing three cases, including Case 2, Case 3, and Case 4. In Case 2, one SOPs device, two capacitors, and three DGs are simultaneously placed. In Case 3, two capacitors and three DGs are simultaneously placed. In Case 4, the results of Case 3 are reapplied, and then one more SOPs device is optimally placed. In the three cases, the minimum and maximum capacities of the SOPs are 0 and 3 MVA; meanwhile, the limits of capacitors and DGs are 0–2 MVAR and 0–2 MW.

The summary of fifty trial runs from the applied algorithms is reported in Fig. 8. In general, EO and COOT can reach the smallest power loss for the three cases, whereas the power loss of CFPSO and TSA is the worst among the algorithms. However, the stabilization of EO is better than COOT's. EO has a smaller height of the three boxes than CFPSO, TSA and COOT. In addition, the whisker of EO is also shorter than others'. Thus, EO is the most suitable algorithm for optimizing the SOPs, capacitors, and DGs in the IEEE 69-node RDN.

The best power loss from EO for Cases 2, 3, and 4 are 18.324, 5.25, and 4.39 kW. The losses on all branches for the cases are plotted in Fig. 9. The branch losses in Case 2 are the highest among the three cases, whereas those in Case 4 are slightly smaller than Case 3. The node voltages are plotted in Fig. 10. Node voltages in all cases are between the minimum and maximum limits of 0.9 and 1.0 Pu, in which the voltage profile of the base case is the closest to the minimum limit and that of Case 4 is the closest to the maximum limit. It means the order of voltage effectiveness is ranked 1, 2, 3, and 4 for Case 4, Case 3, Case 2, and the base case. Case 2 can reach the lowest power loss and the best voltage profile.

Table 8 presents the optimal location and size of added DGs, capacitors and SOPs in the IEEE 69-node system. The parameters indicate that simultaneous placement of the three added component types (i.e., Case 2) just selected two DGs with very low capacity, 706.77 kW 0.15 kW but used a high-capacity SOPs device of 2.35 MVA. Case 4 used the predetermined DGs and capacitors in Case 3 and selected a very small-capacity SOPs device of 0.52 MVA. However, Case 4 reached the smallest power loss as discussed above. Thus, the simultaneous placement of DGs, capacitors and SOPs is not effective.

3.2.3. Case 5: Optimal operation of SOPs and SCBs for one year

In Case 5, we used the optimal solution obtained in Case 4 to simulate the operation of the IEEE 69-node system over one year. However, renewable energies are employed in the case to investigate the effectiveness of the added SOPs device in moving active power and supplying reactive power. Two DGs at nodes 11 and 18 are replaced with solar photovoltaic units (PV1 and PV2), while another DG at node 61 is replaced with a wind turbine (WT). Two shunt capacitors at nodes 61 and 17 (SCB1 and SCB2) and the SOPs device on Line L4 (SOP) remained unchanged but the capactor sizes are optimized simultaneously with the sizes of SOPs, the maximum capacitor sizes of SCB1 and SCB2 are chosen 1350 kVAR and 450 kVAR, respectively [59]. The rated powers of WT, PV1 and PV2 are approximately selected to be 2 MW, 500 kW and 400 kW. The modified IEEE 69-node system with the added electric components is plotted in Fig. 11.

The WT's parameters are taken from Ref. [60] meanwhile its power is calculated by Ref. [61]:

$$P_{WT} = \frac{1}{2}\rho C_P \pi R^2 (V_{wind})^3 \tag{26}$$

In the equation, $C_P = 41.1\%$ is the coefficient of performance (efficiency factor, in percent), $\rho = 1.225\ (kg/m^3)$ is the air density, R = 38.3 (m) is the blade length. V_{wind} is the wind speed (in meter per second). The hourly wind speed index for twelve months in a year

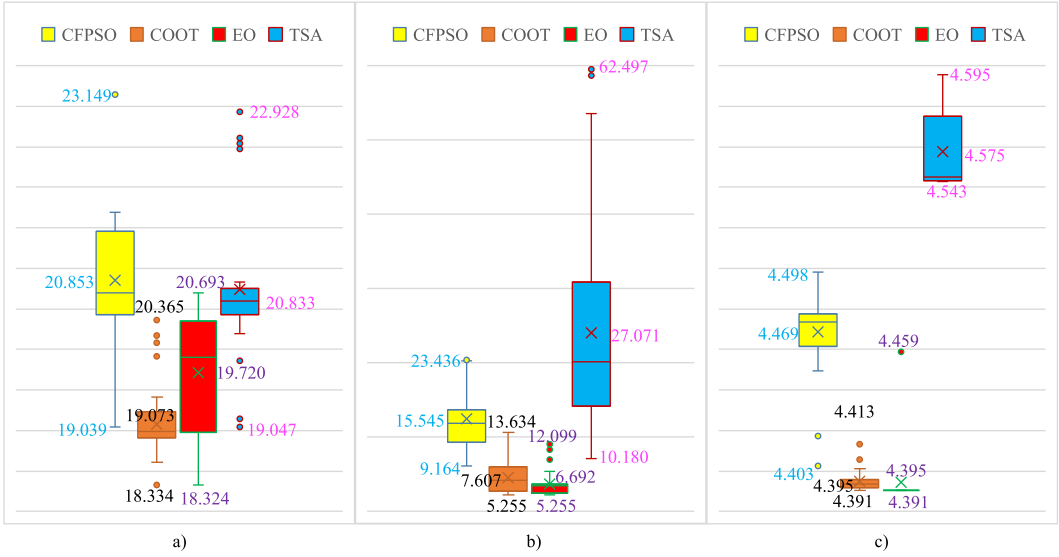

Fig. 8. Total power losses obtained for: a) Case 2, b) Case 3, and c) Case 4.

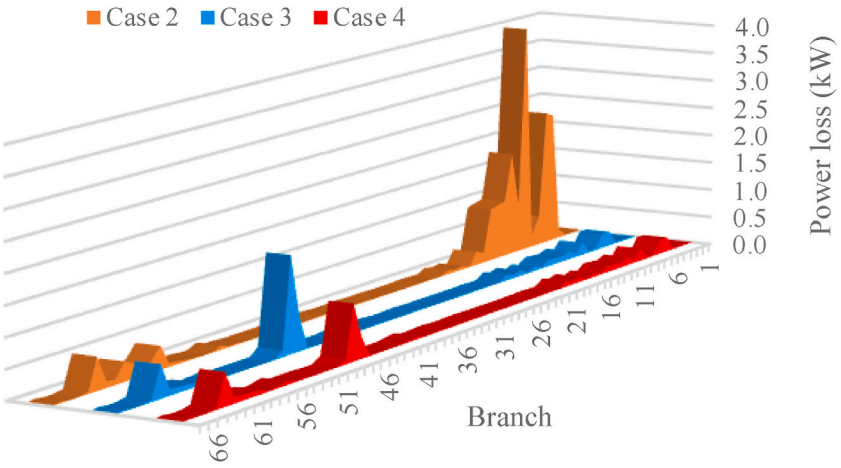

Fig. 9. Power losses on branches for Case 2, Case 3 and Case 4 obtained by EO.

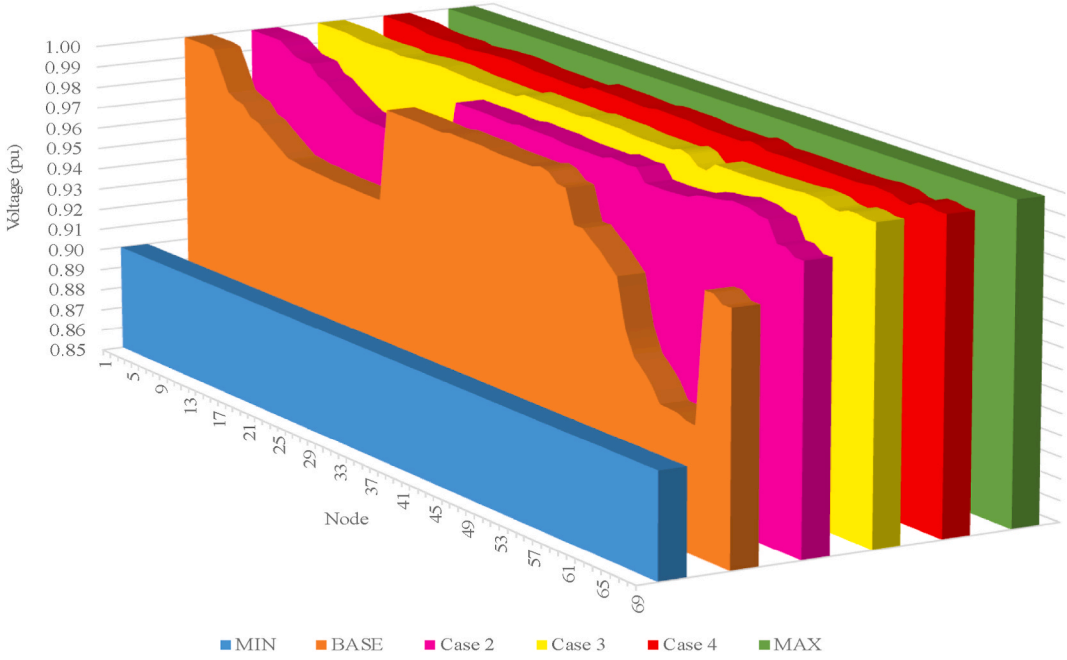

Fig. 10. Voltage at nodes for systems in base case, Case 2, Case 3 and Case 4.

Table 8
Location and size of the added SOPs, capacitors and DGs.

Case	DGs		capacitors		SOPs	
	Location	Size (kW)	Location	Size (kVAR)	Line	Size (MVA)
2	5; 50; 2	0; 706.77; 0.15	50; 22	471.74; 100.87	L6	$S_{VSC,61} = 2.24$ $S_{VSC,2} = 2.35$
3	61;	1674.56;	61;	1238.18;	–	–
4	18; 11	379.56; 494.91	17	352.98	L4	$S_{VSC,59} = 0.05$ $S_{VSC,50} = 0.52$

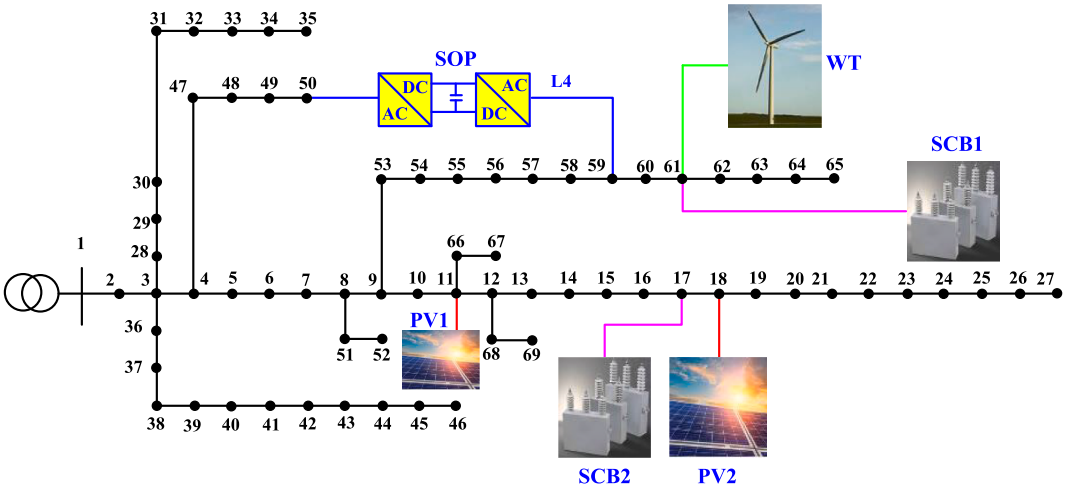

Fig. 11. The modified IEEE 69-node system in Case 5.

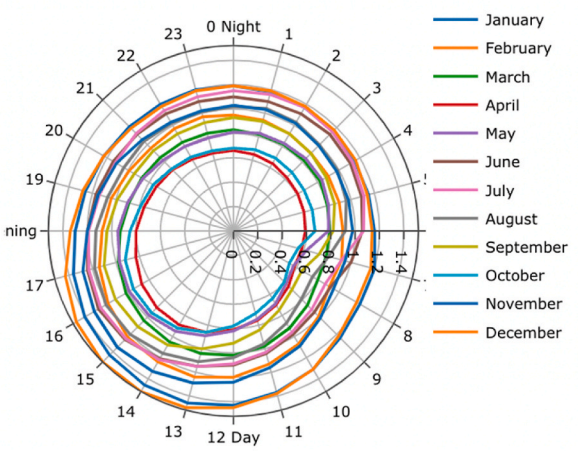

Fig. 12. Wind speed index at 11.420764°, 108.751679°, Tuy Phong District, Binh Thuan Province, Vietnam.

were collected at geographical coordinates 11.420764° and 108.751679° in Tuy Phong District, Binh Thuan Province, Vietnam. The index values are given in Fig. 12 and taken from the website https://globalwindatlas.info/fr. By using the mean wind speed of 10.27 m/s at the height of 100 m, the hourly wind speeds were calculated and reported in Fig. 13. By using a 2-MW wind turbine, the obtained wind power is reported in Fig. 14.

For collecting the solar radiations of PV1 and PV2, the website https://globalsolaratlas.info/map was used for the two locations, Phuoc Dan and Dai Son wards, Ninh Phuoc District, Vietnam. The geographical coordinates of the Phuoc Dan ward are (11°30′55″, 108°52′11″) meanwhile the ward's outside air temperature is 26.8 °C. Dai Son ward's geographical coordinates are 11°35′06″, 108°59′36″, meanwhile, outside air temperature is 26.6 °C. Total area for solar panels of PV1 and PV2 is 6556 and 4734 m^2. The power output of the solar panels (P_{pv}) is determined by Ref. [62]:

$$P_{pv} = \eta.S.SR_{pv}[1 - 0.05(t_0 - 25)] \tag{27}$$

where η describes the conversion efficiency (%) of the PV panels, η = 15% [63]; S is the total area (m^2); SR_{pv} is the solar irradiation (kW/m^2); and t_0 is the outside air temperature (^oC). The solar radiations and power outputs are given in Figs. 15 and 16 for PV1, and Figs. 17 and 18 for PV2.

In addition, the load demands over one year are devided into four seasons, including Spring, Summer, Fall and Winter. The spring has 3 months, it starts from March to May. The summer runs from June to August. From September to November is the Fall. The season that has the lowest days of the year is the Winter, including December, January and February. The load demands in terms of active and reactive power are determined by multiplying the rated demand at load nodes and load factors at hours. The rated demand of loads was taken from the study [15]; meanwhile, the load factors at each hour in the season were taken from the study [64]. The rated load demand and the load factors are given in Figure A1 and Figure A2 in Appendix. We implemented three different scenarios for one year

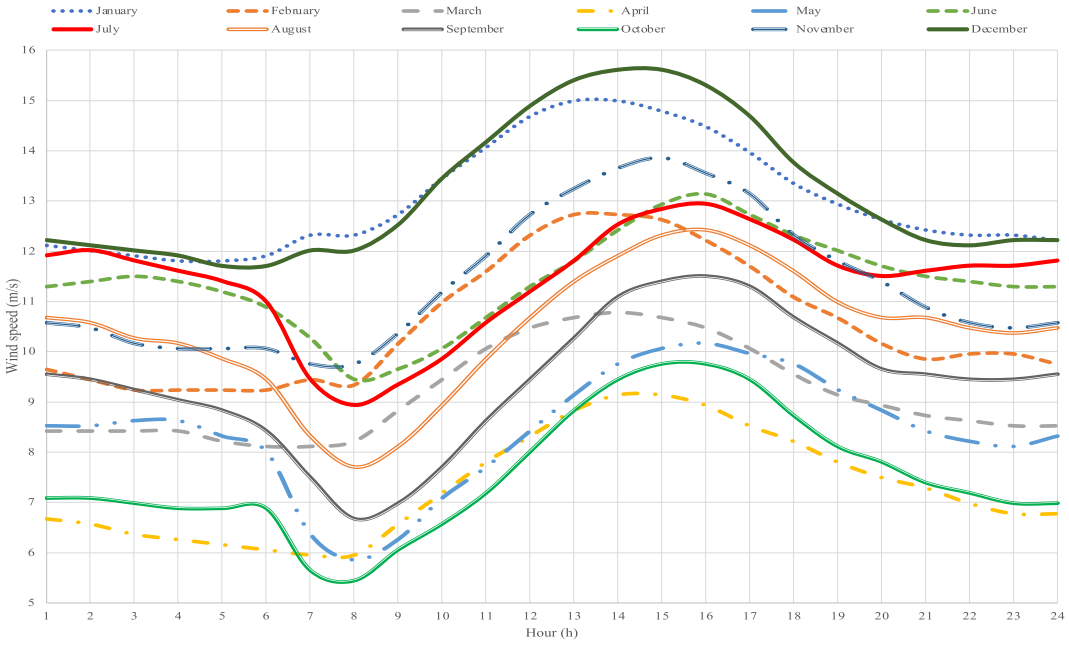

Fig. 13. Hourly wind speeds over twelve months.

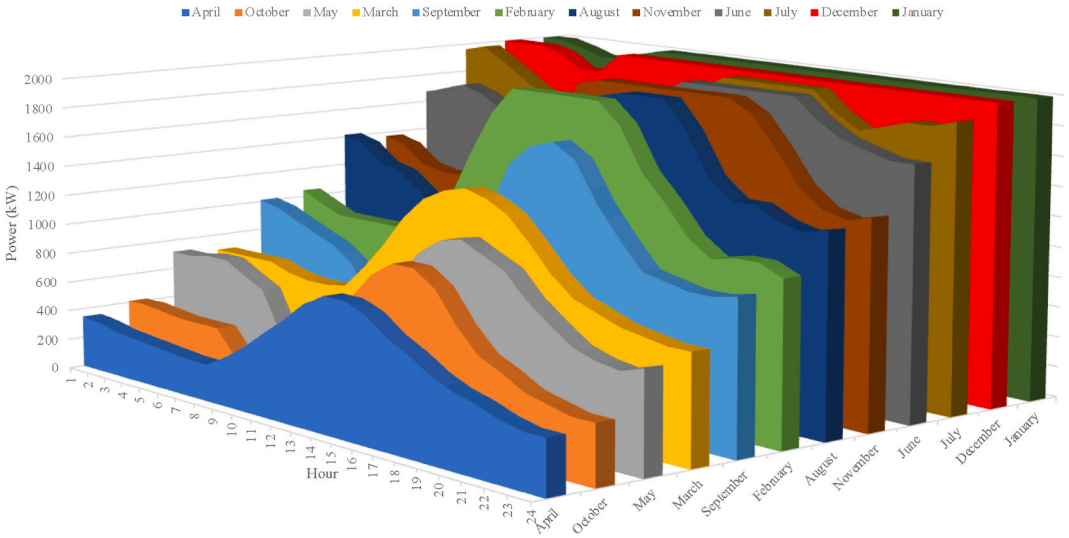

Fig. 14. Hourly power output of the 2-MW wind turbine over twelve months.

operation of the IEEE 69-node system:

Scenario 1: Calculate the total one-year energy losses of the base system without any additional electric components.

Scenario 2: Calculate the total one-year energy losses of Hybrid system 1 with WT, PV1 and PV2.

Scenario 3: Apply EO to reduce the total one-year energy losses of Hybrid system 2 with WT, PV1, PV2, SCB1, SCB2 and SOPs.

EO is not applied in the first two scenarios but in the last scenario. The transformer at node 1 supplies load demand and power loss in Scenario 1; meanwhile, the transformer together with WT, PV1 and PV2 supply to load demand and power loss. So, we just run forward/backward sweep technique to find branch currents and calculate total energy loss. In Scenario 3, we control the reactive and active power flows from the renewable sources and capacitors by using EO to find the SOPs device's parameters. The obtained results are reported in Tables in Appendix. The hourly optimal apparent powers of the SOPs' terminal at node 59 and node 50 are reported in Figure A3 and Figure A4. Hourly optimal generations of SCB1 at node 61 and SCB2 at node 17 are reported in Figure A5 and Figure A6. The detail of hourly energy loss for twelve months is reported in Figure A7.

Comparisons of the energy losses of the twelve months in the base system, Hybrid system 1 and Hybrid system 2 are reported in

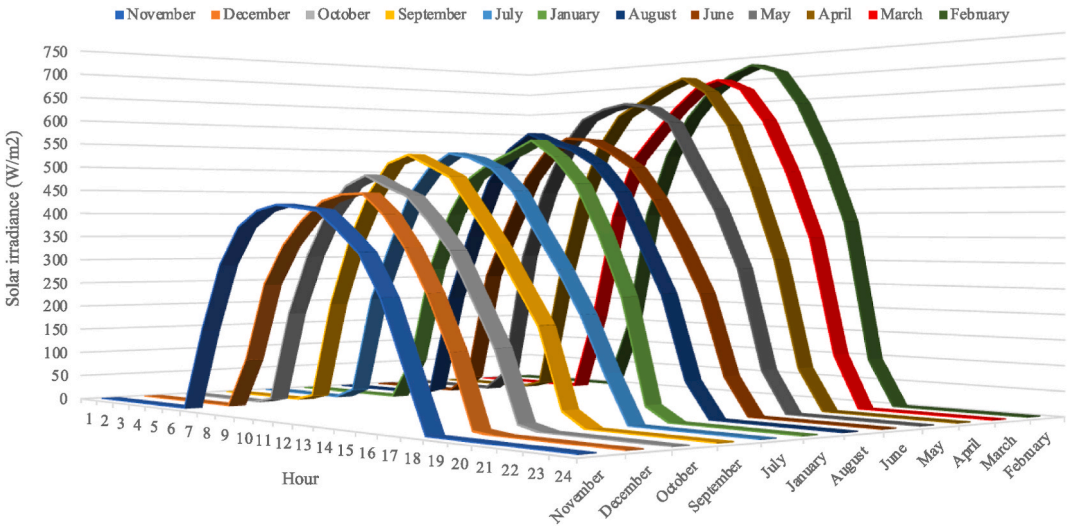

Fig. 15. Hourly solar irradiance of PV1 over twelve months.

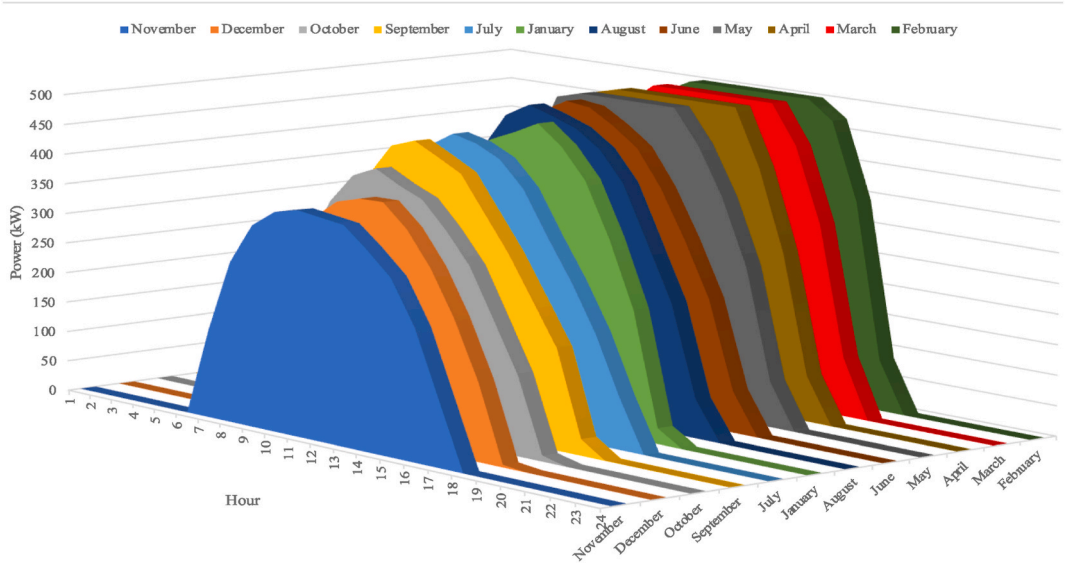

Fig. 16. Hourly power output of PV1 over one year.

Fig. 19. In general, Hybrid system 2 has lower energy losses than the base system and Hybrid System 1 for every month of the year. The monthly energy losses of Hybrid system 2 fluctuated lowly from 154.693 kWh in September to 364.465 kWh in April. In contrast, those of other systems fluctuate highly, from 1228.709 to 3786.249 kWh in the base system and from 574.753 to 1470.842 kWh in Hybrid system 1. The total one-year energy losses of the base system, Hybrid system 1, and Hybrid system 2 are, 753,300.049 kWh, 359,370.914 kWh, and 93,106.277 kWh. Hybrid system 2 can reach smaller total energy losses than the Base system and Hybrid system 1 by 660,193.772 kWh and 266,264.637 kWh. The total energy losses of the base system and hybrid system 1 are 8.1 and 3.9 times those of hybrid system 2. The energy loss reduction can be converted into money by using the energy loss price of 60 $/MWh [65]. As a result, Hybrid system 2 can save $39,612 and $15,976 compared to the base system and Hybrid system 1 for one year.

3.3. Discussions on the SOPs devices' impacts on the system with renewable energies

The section investigates the performance of SOPs in reducing hourly power loss and total energy losses in a year. We chose two different months, January and April, to report power supplied by the transformer at Node 1 and hour power loss. Fig. 20 shows the losses in January and April. The power demand of loads and the power supplied by the transformer of systems is expressed by using the left vertical axis; meanwhile, the power losses of the systems are expressed by using the right vertical axis. The deviation between the

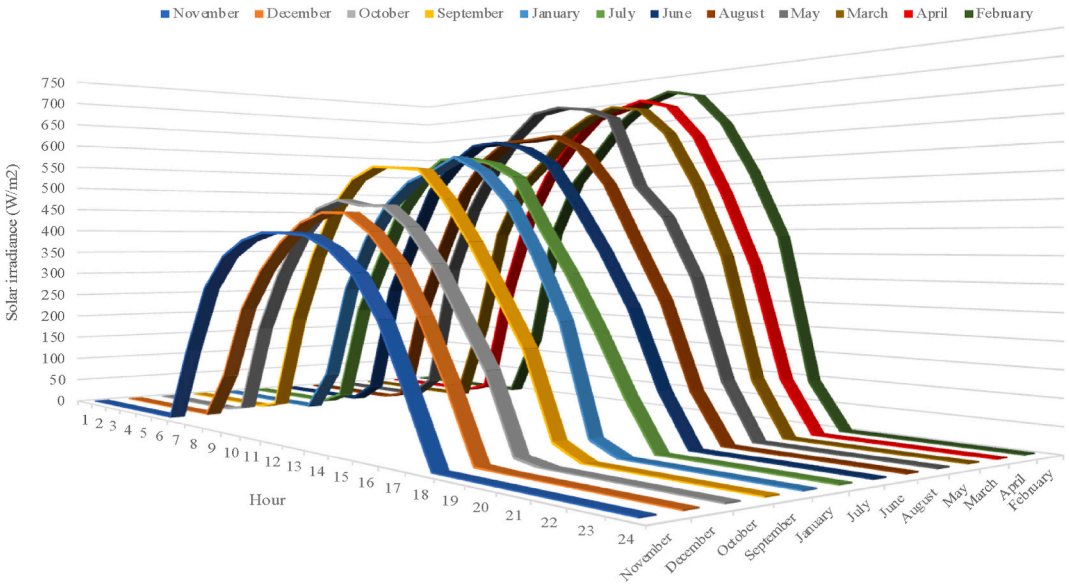

Fig. 17. Hourly solar irradiance of PV2 over twelve months.

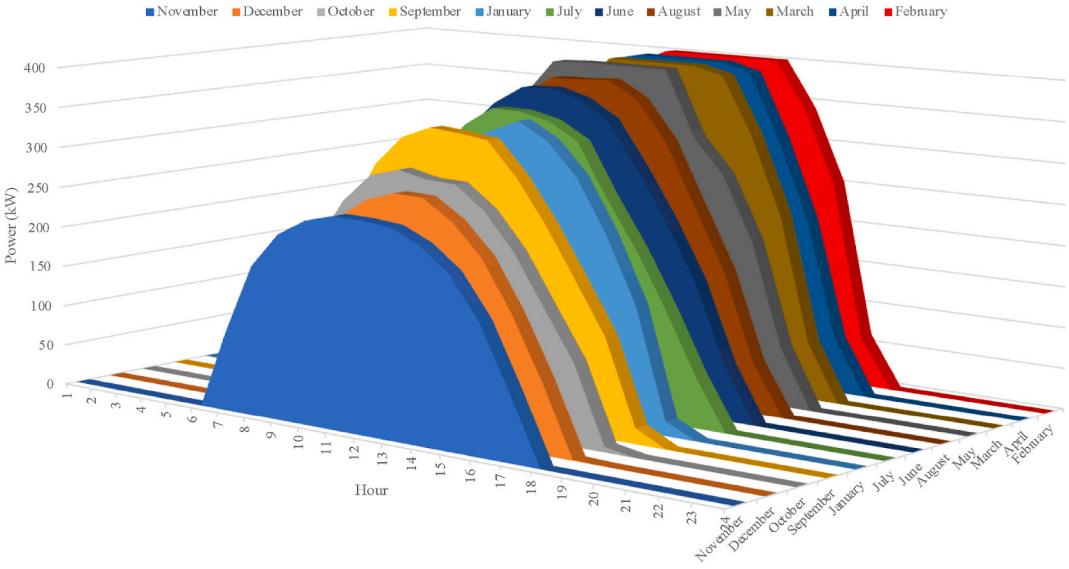

Fig. 18. Hourly power output of PV2 over one year.

two cases is extremely high, so the left vertical axis uses high values, bigger than 3000 kW, and the right vertical axis uses smaller values, about 100 kW. The power supplied by the transformer is calculated using (Load demand + power loss-renewable power), in which the renewable power is the sum of generations from WT, PV1, and PV2. The renewable power is equal to zero in the base system because wind turbines and solar photovoltaic systems are not installed in the system. In Hybrid system 1 and Hybrid system 2, the renewable power is the same.

In Fig. 20a, Hybrid system 2 finds smaller power losses than the base system and Hybrid system 1 for all hours, but Hybrid system 1 suffers higher power losses than the base system at hours 1–6 and 23–24. The power losses of Hybrid system 2 are under 20 kW per hour, but those are around 60 kW in Hybrid system 1 and from under 40 to greater than 100 kW in the base system. Hybrid system 2 can reduce power loss effectively on all days in January. The power supplied by the transformer is negative at hours 1–8, 10–15, and 24 in Hybrid system 1, and at hours 1–16, 23–24 in Hybrid system 2. It means that renewable energy is greater than the sum of load demand and loss at the hours, and it is correct to pay attention to the renewable power and load demand. The yellow curve is above the blue curve at the mentioned hours. In Fig. 20b, the yellow curve is below the blue curve at all hours, and the black curve is always below the dot green curve at all hours. This means that the renewable power is smaller than the load demand, and Hybrid system 1

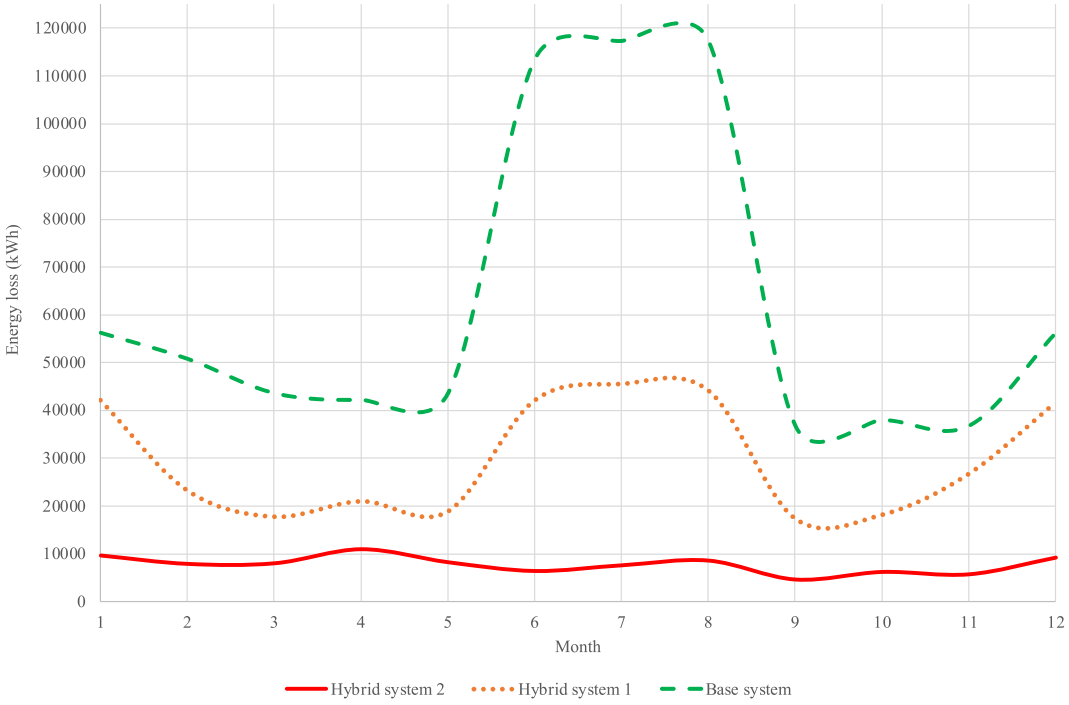

Fig. 19. Monthly energy loss of systems.

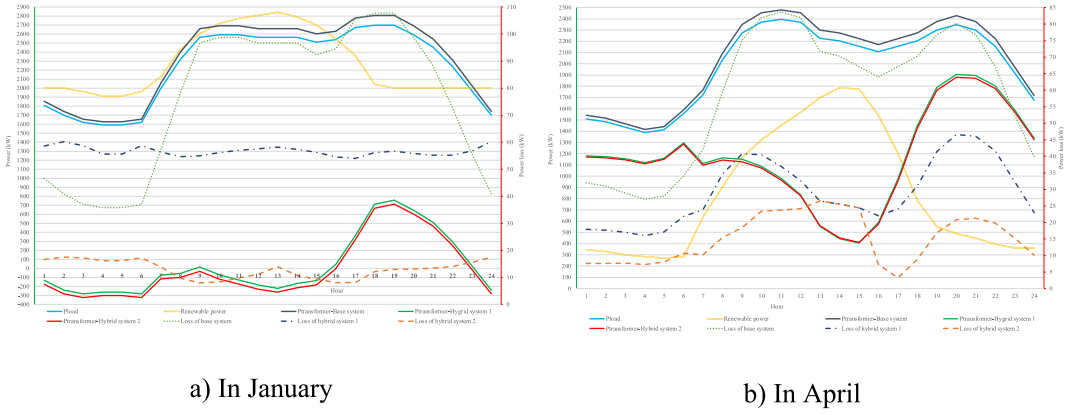

Fig. 20. Comparisons of transformer's power and power losses of systems: a) in January and b) in April.

reached smaller losses than the base system at all hours in April. The power supplied by the transformer in the three systems is always positive. The losses of Hybrid system 2 are smaller than those of the base system at all hours, but the manner is not the same as comparing Hybrid system 2 to Hybrid system 1. In fact, Hybrid system 2 effectively reaches smaller losses at hours 1–12,16-24, but it suffered the same losses at hours 13–15 as Hybrid system 1. EO failed to control active and reactive power flows of the SOPs to reduce power loss at the hours in Hybrid system 2 when renewable power got the highest values in the day.

Similarly, the power losses in March and May in Fig. 21 have the same manner as in April. Hybrid system 2 also has the same losses at hours 13–15 as Hybrid system 1 in March and May, as shown in Fig. 21. The losses of the base system are the highest at all hours; meanwhile, Hybrid system 2 reaches smaller losses than Hybrid system 1 for almost all hours, excluding hours 13–15, when the two systems have the same losses. Verifying the optimal operation parameters of SCB1, SCB2, and SOPs in March, April, and May indicates that the three electric components were set to 0 MW and 0 MVAr for SOPs, and 0 MVAr for SCB1 and SCB2. During the special hours, Hybrid system 2 and Hybrid system 1 are the same, and this is the cause of the same losses.

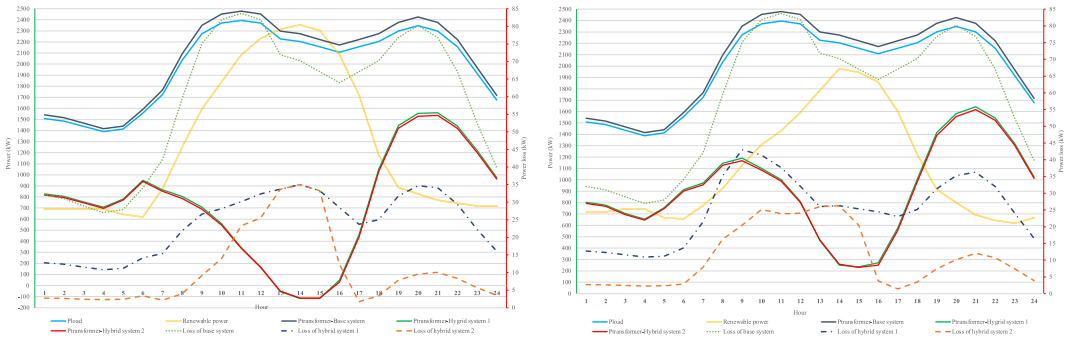

a) In March b) In May

Fig. 21. Comparisons of transformer's power and power losses of systems in two months: a) March and b) May.

3.4. Discussion on challenges and proposed solutions

The study considered the optimal placement and operation of electric components in distribution power grids. The determination of location and capacity for Capacitors, DGs, and SOPs devices was implemented in the optimal design problem, whereas the determination of operating parameters for SOPs and Capacitors was implemented in the optimization operation problem. The location and capacity of Capacitors, DGs, and SOPs devices were found based on the peak load demand and the data of the distribution power system. Then, we replaced two DGs with two solar radiation-based DGs and one wind-based DG. In the optimal design problem, the accuracy of the peak load demand and the gird's data has a significant impact on the found location and capacity of DGs, capacitors, and SOPs devices. In practice, load demand and renewable power cannot be 100% accurate as predicted and obtained from the wind and solar global atlas. So, optimal solutions obtained by using optimization algorithms cannot be applied at each hour for a practical distribution power network. Furthermore, the inexact data influences the design problem of placing renewable power sources, i.e., selecting the location to install renewable power sources and selecting the capacity of renewable power sources. Previous studies coped with the same big problem, and they have yet to find an absolute solution for determining the exact power of renewable energy and load demand at each hour.

The study neglected the power loss in conductors connecting two nodes where SOPs devices were placed optimally. The power loss depends on the conductors' resistance and operating current. The resistance is dependent on the length and area of the conductors. The length is the distance between two nodes; meanwhile, the area is dependent on the rated power of the SOPs. The selection of the conductors' area and the current is simple by using the rated power of SOPs; however, the calculation of the conductors' length is the greatest challenge faced by the study. The available data of the two standard IEEE distribution power networks were only the load demand, resistance, and reactance of lines, whereas the important distance was ignored. Derived from the reason, previous studies based on the standard IEEE networks have had the same limitations of neglecting the distance. So, the study proposes a solution to the problem with three steps as follows.

- Consider a practical distribution power network with existing solar photovoltaic systems to place SOPs devices optimally. A geographical atlas is used to determine the exact distance between each two nodes.
- Use high-performance metaheuristic algorithms to determine the most, the second most, the third, and the fourth suitable connections to place one SOPs device. Each connection comprises two unconnected nodes in the existing network configuration.
- Survey geographical information of the found nodes in the practical distribution power networks to determine the connection that can be implemented for placing the SOPs device.

In the case that input data are 100% accurate, the placement and operation of the electric components can reach higher achievements. Solutions obtained by running applied algorithms are also highly reliable. After having highly accurate data and optimal solutions, the forward/backward sweep technique is run to solve the power flows, and the results obtained for standard IEEE and practical distribution power grids are highly accurate.

4. Conclusions

This paper applied EO to optimize the placement of shunt capacitors, distributed generators, and soft open points in distribution power networks. The paper's task was to find the location for installing the added components and determine their capacity for reducing power loss of a single hour and the total energy losses of one year. In the IEEE 33-node DPN, Case 1 optimized the placement of three DGs and Case 2 optimized five SOPs devices and three DGs. In the IEEE 69-node DPN, five study cases were implemented. Case 1 optimized the capacity of SOPs devices on eight determined lines. Case 2 optimized the placement of one SOPs and several capacitors and DGs. Case 3 only optimized the placement of capacitors and DGs. Case 4 used the optimal placement of capacitors and DGs in Case

3 and optimized one more SOPs device. Case 5 considered the optimization operation of capacitors and SOPs over one year for three systems: a base system without any additional electric components, Hybrid system 1 with renewable energies, and Hybrid system 2 with renewable energies, shunt capacitor banks and soft open points device. In Case 5, three DGs in Case 4 were replaced with one 2-MW wind turbine, one 500-kW solar photovoltaic system, and one 400-kW solar photovoltaic system. In addition, data on wind speed and solar radiation from the earth were used to calculate wind and solar power at each hour over one year. The power demand of each load at each hour was calculated by using the rated demand and load factors over four seasons. The contributions of the paper are summarized as follows.

- Find out EO, which was the most effective algorithm reaching lower power losses than three applied algorithms (CFPSO, COOT and TSA) and other previous algorithms (PSO [53], TM [54], MOTA [54], BA [55], HSA [56], LSPSO [15], MPSO [13], CSA [13], AO [13], and DSSA [13]).
- For the first system, EO reached a loss reduction of 65.34%, while others got a reduction from 49.52% to 65.34% compared to the base system in Case 1. EO reached a loss reduction of 97.29%, while others are from 79.5% to 97.22% compared to the base system.
- In Case 1 of the second DPN, the study reached a smaller power loss than previous studies, from 19.39 to 40.19 kW.
- In other cases of the second DPN, the study could reach a smaller power loss than the base system by 206.686, 219.76, and 220.62 kW, which are nearly equal to the base system's.
- By placing renewable energies, capacitors, and SOPs devices in the second DPN, the obtained solution could reach a smaller one-year energy loss than the base system by 266,264.637 kWh and the modified system with renewable energies by 660,193.772 kWh. Accordingly, the study could benefit more than the base and modified systems with renewable energies by $39,612 and $15,976, respectively.
- Indicating that using capacitors and SOPs could not reach smaller losses for all operation times in the second system with renewable energies. At hours 13–15 in Spring, capacitors and SOPs were set to 0 MVAr and 0 MVA to reach the same losses as the system without capacitors and SOPs.

The study had significant contributions to power systems in cutting power and energy losses and using the high penetration of renewable energies; however, it still had huge limitations. The certainty of wind and solar power generation was considered over one year; however, the estimated wind speeds and solar radiation, and given load demand for every single period within 1 h, were not wholly exact. In practice, the load and the renewable data can change many times over 1 h. So, obtained solutions to the distribution power network operation problem cannot be applied for each hour. On the other hand, the study did not consider real distribution networks with SOPs devices, capacitors, and renewable distributed generators. The investment and operating costs, as well as the technology and regulations of the added electric components, should have been taken into account when optimizing their capacity and operating parameters. A practical distribution power grid with available capacitors, renewable distributed generators, and SOPs devices will be considered in future work. The investment and operating costs will be taken into account in objective functions for solving the optimal design problem determining the capacity and the number of added electric components. The technology and regulations of the added electric component will be considered in the optimization operation problem to determine the operating parameters of these electric components. Indeed, future studies will be able to reach practical results and more significant benefits for applied distribution power networks.

Data availability

Data will be made available on request.

CRediT authorship contribution statement

Hai Van Tran: Writing – original draft, Software. **Anh Viet Truong:** Validation, Supervision, Conceptualization. **Tan Minh Phan:** Resources, Methodology, Data curation. **Thang Trung Nguyen:** Writing – review & editing, Supervision, Methodology, Investigation.

Declaration of competing interest

The authors declare that they have no known competing financial interests or personal relationships that could have appeared to influence the work reported in this paper.

Acknowledgements

The authors warmly thank Ho Chi Minh City University of Technology and Education, Ho Chi Minh City University of Industry and Trade, and Ton Duc Thang university. The universities have supported the authors software, rooms and other good conditions to finish the study.

APPENDIX

Table A1
Data of the IEEE 33-node DPN

No. line	From node	To node	Resistance (Ω)	Reactance (Ω)	Full load	
					P (kW)	Q (kVAr)
1	1	2	0.0922	0.047	100	60
2	2	3	0.4930	0.2511	90	40
3	3	4	0.3660	0.1864	120	80
4	4	5	0.3811	0.1941	60	30
5	5	6	0.8190	0.707	60	20
6	6	7	0.1872	0.6188	200	100
7	7	8	0.7114	0.2351	200	100
8	8	9	1.0300	0.74	60	20
9	9	10	1.0440	0.74	60	20
10	10	11	0.1966	0.0650	45	30
11	11	12	0.3744	0.1238	60	35
12	12	13	1.4680	1.1550	60	35
13	13	14	0.5416	0.7129	120	80
14	14	15	0.5910	0.526	60	10
15	15	16	0.7463	0.5450	60	20
16	16	17	1.2890	1.721	60	20
17	17	18	0.7320	0.5740	90	40
18	2	19	0.1640	0.1565	90	40
19	19	20	1.5042	1.3554	90	40
20	20	21	0.4095	0.4784	90	40
21	21	22	0.7089	0.9373	90	40
22	3	23	0.4512	0.3083	90	50
23	23	24	0.8980	0.7091	420	200
24	24	25	0.8960	0.7011	420	200
25	6	26	0.2030	0.1034	60	25
26	26	27	0.2842	0.1447	60	25
27	27	28	1.0590	0.9337	60	20
28	28	29	0.8042	0.7006	120	70
29	29	30	0.5075	0.2585	200	600
30	30	31	0.9744	0.9630	150	70
31	31	32	0.3105	0.3619	210	100
32	32	33	0.3410	0.5302	60	40

Table A2
Data of the IEEE 69-node DPN

No. line	From node	To node	Resistance (Ω)	Reactance (Ω)	Full load	
					P (kW)	Q (kVAr)
1	1	2	0.0005	0.0012	0	0
2	2	3	0.0005	0.0012	0	0
3	3	4	0.0015	0.0036	0	0
4	4	5	0.0251	0.0294	0	0
5	5	6	0.366	0.1864	2.6	2.2
6	6	7	0.3811	0.1941	40.4	30
7	7	8	0.0922	0.047	75	54
8	8	9	0.0493	0.0251	30	22
9	9	10	0.819	0.2707	28	19
10	10	11	0.1872	0.0691	145	104
11	11	12	0.7114	0.2351	145	104
12	12	13	1.03	0.34	8	5.5
13	13	14	1.044	0.345	8	5.5
14	14	15	1.058	0.3496	0	0
15	15	16	0.1966	0.065	45.5	30
16	16	17	0.3744	0.1238	60	35
17	17	18	0.0047	0.0016	60	35
18	18	19	0.3276	0.1083	0	0
19	19	20	0.2106	0.069	1	0.6
20	20	21	0.3416	0.1129	114	81
21	21	22	0.014	0.0046	5.3	3.5
22	22	23	0.1591	0.0526	0	0
23	23	24	0.3463	0.1145	28	20

(*continued on next page*)

Table A2 (*continued*)

No. line	From node	To node	Resistance (Ω)	Reactance (Ω)	Full load	
					P (kW)	Q (kVAr)
24	24	25	0.7488	0.2745	0	0
25	25	26	0.3089	0.1021	14	10
26	26	27	0.1732	0.0572	14	10
27	3	28	0.0044	0.0108	26	18.6
28	28	29	0.064	0.1565	26	18.6
29	29	30	0.3978	0.1315	0	0
30	30	31	0.0702	0.0232	0	0
31	31	32	0.351	0.116	0	0
32	32	33	0.839	0.2816	14	10
33	33	34	1.708	0.5646	19.5	14
34	34	35	1.474	0.4673	6	4
35	3	36	0.0044	0.0108	26	18.55
36	36	37	0.064	0.1565	26	18.55
37	37	38	0.1053	0.123	0	0
38	38	39	0.0304	0.0355	24	17
39	39	40	0.0018	0.0021	24	17
40	40	41	0.7283	0.8509	1.2	1
41	41	42	0.31	0.3623	0	0
42	42	43	0.041	0.0478	6	4.3
43	43	44	0.0092	0.0116	0	0
44	44	45	0.1089	0.1373	39.22	26.3
45	45	46	0.0009	0.0012	39.22	26.3
46	4	47	0.0034	0.0084	0	0
47	47	48	0.0851	0.2083	79	56.4
48	48	49	0.2898	0.7091	384.7	274.5
49	49	50	0.0822	0.2011	384	274.5
50	8	51	0.0928	0.0473	40.5	28.3
51	51	52	0.3319	0.1114	3.6	2.7
52	9	53	0.174	0.0886	4.35	3.5
53	53	54	0.203	0.1034	26.4	19
54	54	55	0.2842	0.1447	24	17.2
55	55	56	0.2813	0.1433	0	0
56	56	57	1.59	0.5337	0	0
57	57	58	0.7837	0.263	0	0
58	58	59	0.3042	0.1006	100	72
59	59	60	0.3861	0.1172	0	0
60	60	61	0.5075	0.2585	1244	888
61	61	62	0.0974	0.0496	32	23
62	62	63	0.145	0.0738	0	0
63	63	64	0.7105	0.3619	227	162
64	64	65	1.041	0.5302	59	42
65	11	66	0.2012	0.0611	18	13
66	66	67	0.0047	0.0014	18	13
67	12	68	0.7394	0.2444	28	20
68	68	69	0.0047	0.0016	28	20

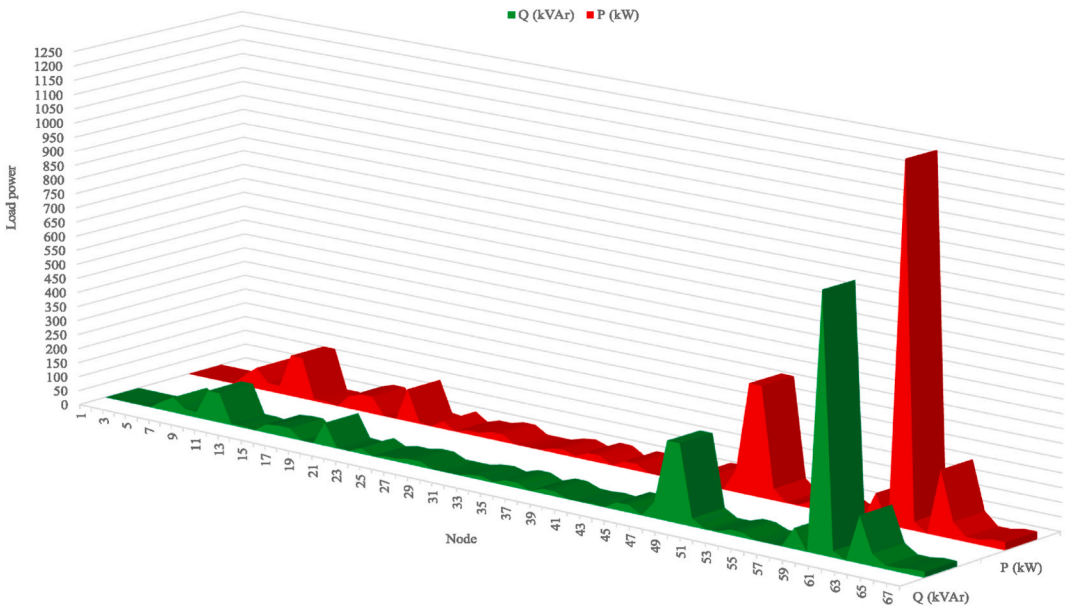

Fig. A1. Load demand at nodes in the IEEE 69-node system.

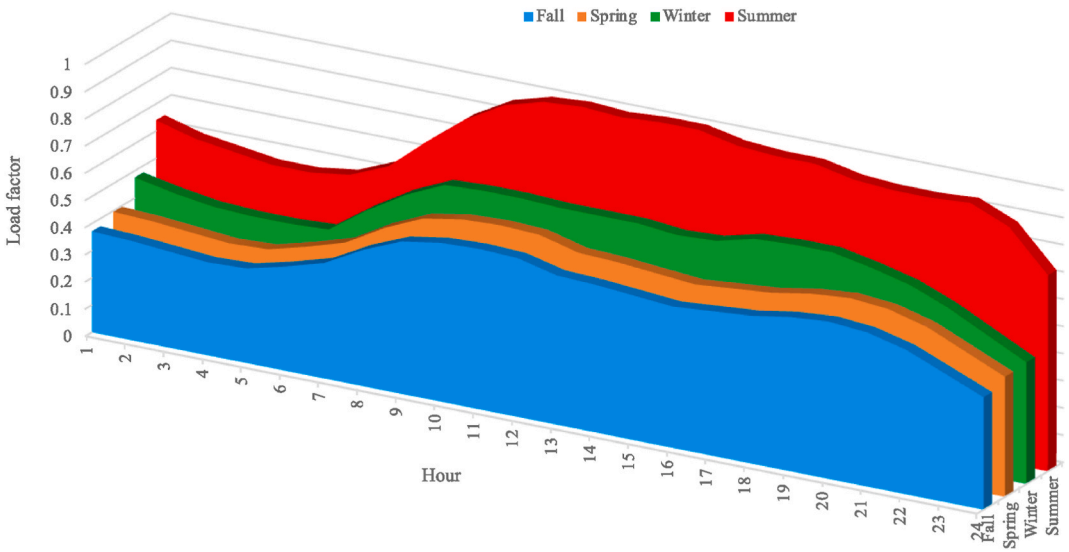

Fig. A2. Hourly load factors for days in four seasons.

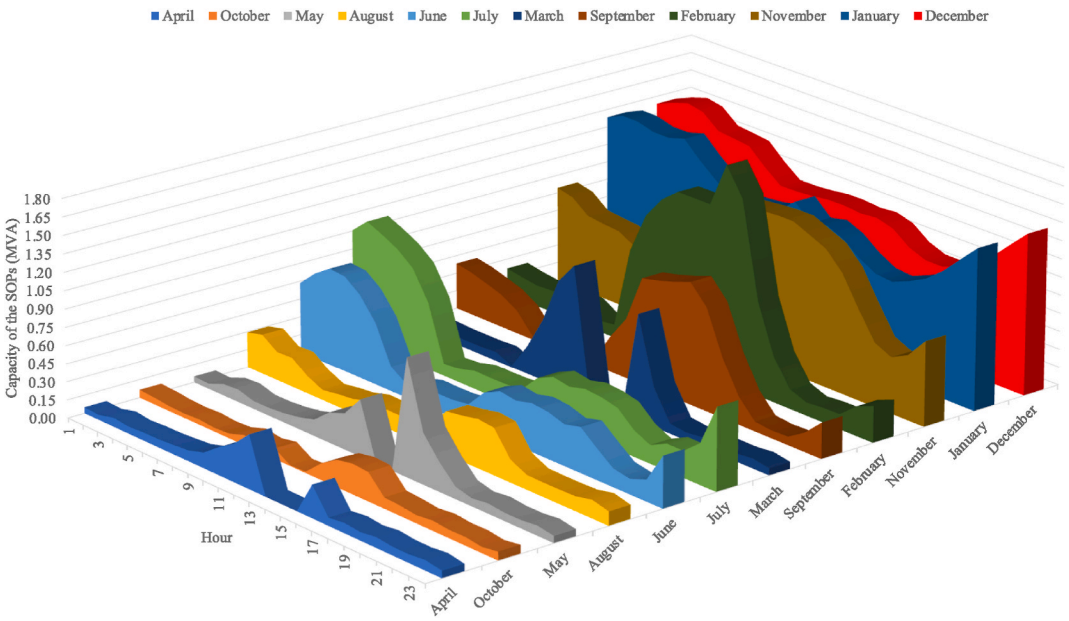

Fig. A3. Hourly optimal apparent power of the SOPs at node 59 ($S_{VSC,59}$).

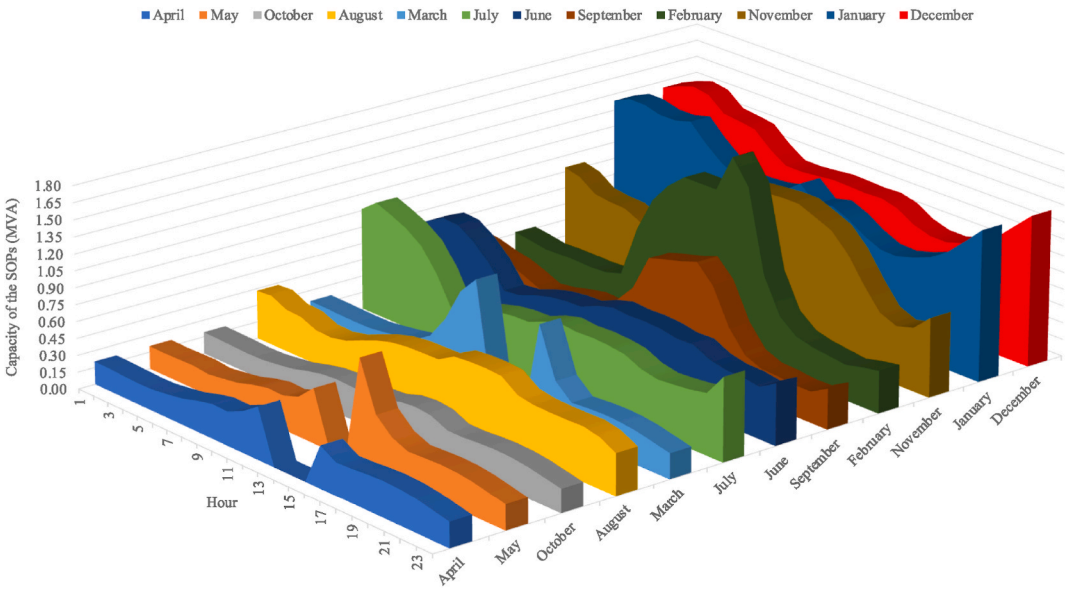

Fig. A4. Hourly optimal apparent power of the SOPs at node 50 ($S_{VSC,50}$).

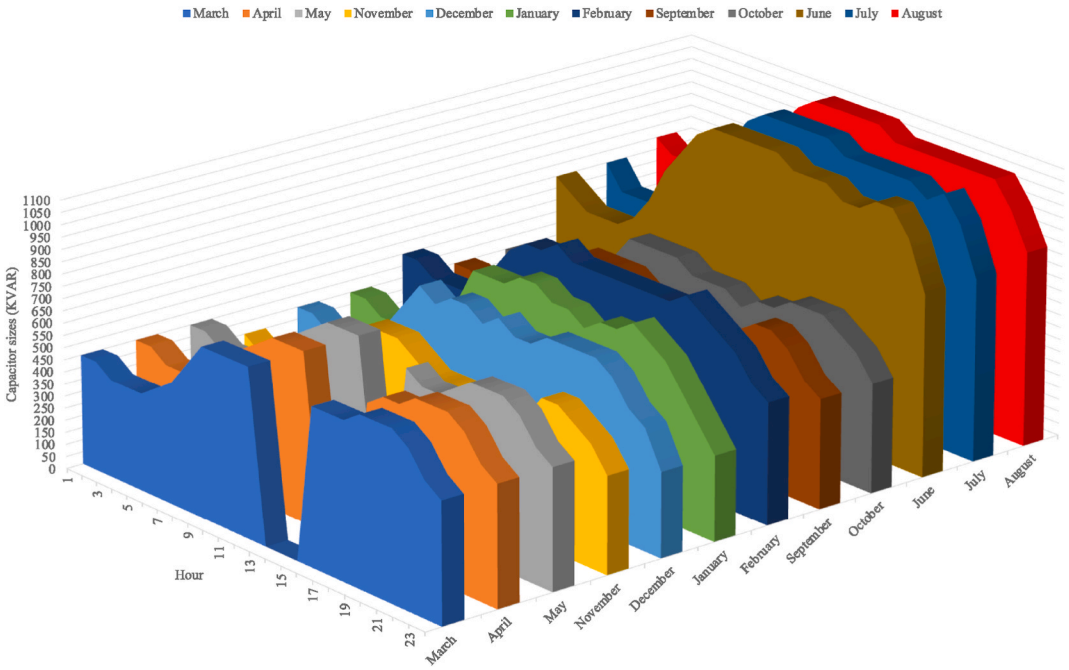

Fig. A5. Hourly optimal generation of SCB1 at node 61 over 12 months.

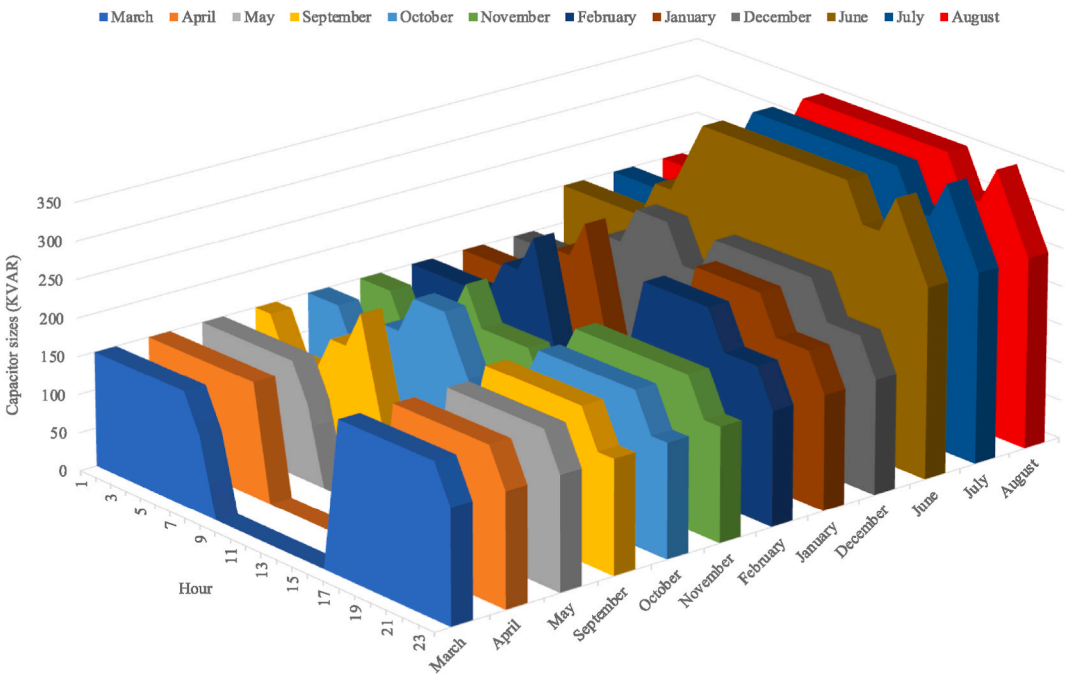

Fig. A6. Hourly optimal generation of SCB2 at node 17 over 12 months.

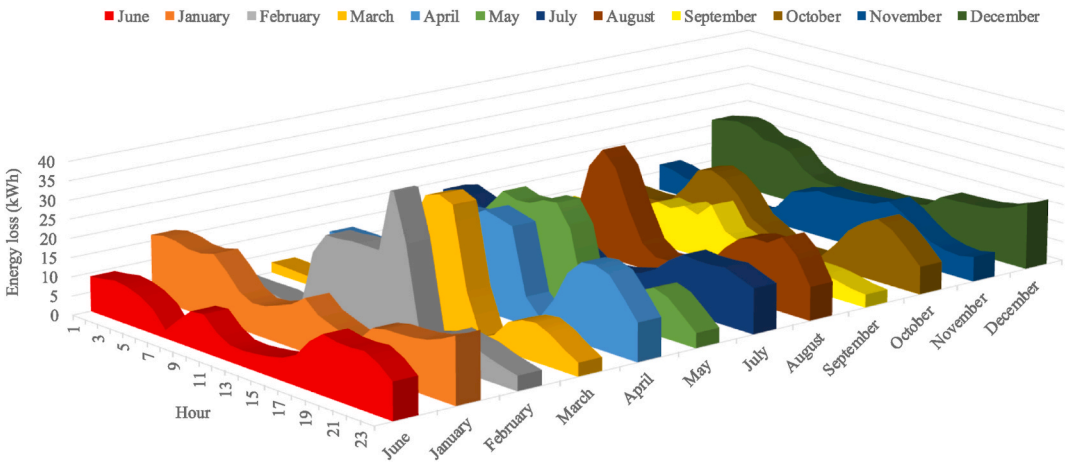

Fig. A7. Hourly energy loss of Hybrid system 2 for twelve months.

References

[1] Y.H. Song, G.S. Wang, A.T. Johns, P.Y. Wang, Distribution network reconfiguration for loss reduction using fuzzy controlled evolutionary programming, IEE Proc. Generat. Transm. Distrib. 144 (4) (1997) 345–350, https://doi.org/10.1049/ip-gtd:19971101.

[2] K.E. Okedu, A. Al Abri, Effects of solar photovoltaic penetration on the behavior of grid-connected loads, Math. Probl Eng. 2022 (2022) 1–11, https://doi.org/10.1155/2022/9579437.

[3] T.T. Nguyen, T.T. Nguyen, M.Q. Duong, An improved equilibrium optimizer for optimal placement of photovoltaic systems in radial distribution power networks, Neural Comput. Appl. 34 (2022) 1–30, https://doi.org/10.1007/s00521-021-06779-w.

[4] A. Askarzadeh, Capacitor placement in distribution systems for power loss reduction and voltage improvement: a new methodology, IET Gener., Transm. Distrib. 10 (14) (2016) 3631–3638, https://doi.org/10.1049/iet-gtd.2016.0419.

[5] S. Angalaeswari, P. Sanjeevikumar, K. Jamuna, Z. Leonowicz, Hybrid PIPSO-SQP algorithm for real power loss minimization in radial distribution systems with optimal placement of distributed generation, Sustainability 12 (14) (2020) 5787, https://doi.org/10.3390/su12145787.

[6] Y.M. Atwa, E.F. El-Saadany, Probabilistic approach for optimal allocation of wind-based distributed generation in distribution systems, IET Renew. Power Gener. 5 (1) (2011) 79–88, https://doi.org/10.1049/iet-rpg.2009.0011.

[7] L.C. Kien, T.T. Bich Nga, T.M. Phan, T.T. Nguyen, Coot optimization algorithm for optimal placement of photovoltaic generators in distribution systems considering variation of load and solar radiation, Math. Probl Eng. 2022 (2022) 1–17, https://doi.org/10.1155/2022/2206570.

[8] A.A. Abo El-Ela, S.M. Allam, A.M. Shaheen, N.A. Nagem, Optimal allocation of biomass distributed generation in distribution systems using equilibrium algorithm, International Transactions on Electrical Energy Systems 31 (2) (2021) e12727, https://doi.org/10.1002/2050-7038.12727.

[9] J. Dias Santos, F. Marques, L.P. Garcés Negrete, G.A. Andrêa Brigatto, J.M. López-Lezama, N. Muñoz-Galeano, A novel solution method for the distribution network reconfiguration problem based on a search mechanism enhancement of the improved harmony search algorithm, Energies 15 (6) (2022) 2083, https://doi.org/10.3390/en15062083.

[10] J.M. Bloemink, T.C. Green, Increasing distributed generation penetration using soft normally-open points, IEEE PES General Meeting (2010) 1–8, https://doi.org/10.1109/PES.2010.5589629.

[11] X. Jiang, Y. Zhou, W. Ming, P. Yang, J. Wu, An overview of soft open points in electricity distribution networks, IEEE Trans. Smart Grid 13 (3) (2022) 1899–1910, https://doi.org/10.1109/TSG.2022.3148599.

[12] M. Ismail, E. Hassane, E.M. Hassan, L. Tijani, Power losses minimization in distribution system using soft open point, in: 2020 1st International Conference on Innovative Research in Applied Science, Engineering and Technology (IRASET), 2020, pp. 1–5, https://doi.org/10.1109/IRASET48871.2020.9092002.

[13] H. Nkc, S.R. Inkollu, R. Patil, V. Janamala, Aquila optimizer based optimal allocation of soft open points for multi objective operation in electric vehicles integrated active distribution networks, International Journal of Intelligent Engineering and Systems 15 (4) (2022) 269–278, https://doi.org/10.22266/ijies2022.0831.25.

[14] P. Li, H. Ji, C. Wang, J. Zhao, G. Song, F. Ding, J. Wu, Coordinated control method of voltage and reactive power for active distribution networks based on soft open point, IEEE Trans. Sustain. Energy 8 (4) (2017) 1430–1442, https://doi.org/10.1109/TSTE.2017.2686009.

[15] Q. Qi, J. Wu, C. Long, Multi-objective operation optimization of an electrical distribution network with soft open point, Appl. Energy 208 (2017) 734–744, https://doi.org/10.1016/j.apenergy.2017.09.075.

[16] Y. Zheng, Y. Song, D.J. Hill, A general coordinated voltage regulation method in distribution networks with soft open points, Int. J. Electr. Power Energy Syst. 116 (2020) 105571, https://doi.org/10.1016/j.ijepes.2019.105571.

[17] C. Han, S. Song, Y. Yoo, J. Lee, G. Jang, M. Yoon, Optimal operation of soft-open points for high penetrated distributed generations on distribution networks, in: 2019 10th International Conference on Power Electronics and ECCE Asia (ICPE 2019-ECCE Asia), 2019, pp. 806–812, https://doi.org/10.23919/ICPE2019-ECCEAsia42246.2019.8796910.

[18] W. Cao, J. Wu, N. Jenkins, C. Wang, T. Green, Benefits analysis of Soft Open Points for electrical distribution network operation, Appl. Energy 165 (2016) 36–47, https://doi.org/10.1016/j.apenergy.2015.12.022.

[19] Q. Qi, J. Wu, Increasing distributed generation penetration using network reconfiguration and soft open points, Energy Proc. 105 (2017) 2169–2174, https://doi.org/10.1016/j.egypro.2017.03.612.

[20] I. Diaaeldin, S. Abdel Aleem, A. El-Rafei, A. Abdelaziz, A.F. Zobaa, Optimal network reconfiguration in active distribution networks with soft open points and distributed generation, Energies 12 (21) (2019) 4172, https://doi.org/10.3390/en12214172.

[21] I.M. Diaaeldin, S.H.A. Aleem, A. El-Rafei, A.Y. Abdelaziz, M. Ćalasan, Optimal soft open points operation and distributed generations penetration in a reconfigured Egyptian distribution network, in: 2021 25th International Conference on Information Technology, IT), 2021, pp. 1–6, https://doi.org/10.1109/IT51528.2021.9390150.

[22] M. Ehsanbakhsh, M.S. Sepasian, Simultaneous siting and sizing of Soft Open Points and the allocation of tie switches in active distribution network considering network reconfiguration, IET Gener., Transm. Distrib. 17 (1) (2023) 263–280, https://doi.org/10.1049/gtd2.12683.

[23] S. Alwash, S. Ibrahim, A.M. Abed, Distribution system reconfiguration with soft open point for power loss reduction in distribution systems based on hybrid water cycle algorithm, Energies 16 (1) (2022) 199, https://doi.org/10.3390/en16010199.

[24] P. Li, H. Ji, C. Wang, G. Song, J. Zhao, Y. Song, Robust Operation Strategy of Soft Open Point for Active Distribution Network with Uncertainties, IEEE Power & Energy Society General Meeting, 2017, pp. 1–5, https://doi.org/10.1109/PESGM.2017.8274602, 2017.

[25] H. Ji, C. Wang, P. Li, J. Zhao, G. Song, J. Wu, Quantified flexibility evaluation of soft open points to improve distributed generator penetration in active distribution networks based on difference-of-convex programming, Appl. Energy 218 (2018) 338–348, https://doi.org/10.1016/j.apenergy.2018.02.170.

[26] H. Ji, C. Wang, P. Li, F. Ding, J. Wu, Robust operation of soft open points in active distribution networks with high penetration of photovoltaic integration, IEEE Trans. Sustain. Energy 10 (1) (2018) 280–289, https://doi.org/10.1109/TSTE.2018.2833545.

[27] X. Jiang, W. Ming, Y. Zhou, J. Wu, Optimal operation of soft open points to minimize energy curtailment of distributed generation in electricity distribution networks, Applied Energy Symposium 14 (3) (2021) 1–6, https://doi.org/10.46855/energy-proceedings-7459, 2020.

[28] V.B. Pamshetti, S.P. Singh, Coordinated allocation of BESS and SOP in high PV penetrated distribution network incorporating DR and CVR schemes, IEEE Syst. J. 16 (1) (2020) 420–430, https://doi.org/10.1109/JSYST.2020.3041013.

[29] J. Wang, N. Zhou, A. Tao, Q. Wang, Optimal operation of soft open points-based energy storage in active distribution networks by considering the battery lifetime, Front. Energy Res. 8 (2021) 633401, https://doi.org/10.3389/fenrg.2020.633401.

[30] V. Janamala, K. Radha Rani, P. Sobha Rani, A.N. Venkateswarlu, S.R. Inkollu, Optimal switching operations of soft open points in active distribution network for handling variable penetration of photovoltaic and electric vehicles using artificial rabbits optimization, Process Integration and Optimization for Sustainability 7 (1–2) (2023) 419–437, https://doi.org/10.1007/s41660-022-00304-9.

[31] A. Farzamnia, S. Marjani, S. Galvani, K.T.T. Kin, Optimal allocation of soft open point devices in renewable energy integrated distribution systems, IEEE Access 10 (2022) 9309–9320, https://doi.org/10.1109/ACCESS.2022.3144349.

[32] M.A. Saaklayen, M.N.S.K. Shabbir, X. Liang, S.O. Faried, M. Janbakhsh, A Novel Methodology for Optimal Allocation and Sizing of Soft Open Points in Distribution Networks, IEEE Industry Applications Society Annual Meeting (IAS), 2022, pp. 1–8, https://doi.org/10.1109/IAS54023.2022.9939720.

[33] M.A. Saaklayen, M.N.S.K. Shabbir, X. Liang, S.O. Faried, M. Janbakhsh, A two-stage multi-scenario optimization method for placement and sizing of soft open points in distribution networks, IEEE Trans. Ind. Appl. 59 (3) (2023) 2877–2891, https://doi.org/10.1109/TIA.2023.3245588.

[34] C. Long, J. Wu, L. Thomas, N. Jenkins, Optimal operation of soft open points in medium voltage electrical distribution networks with distributed generation, Appl. Energy 184 (2016) 427–437, https://doi.org/10.1016/j.apenergy.2016.10.031.

[35] M.A. Abdelrahman, C. Long, J. Wu, N. Jenkins, Optimal operation of multi-terminal soft open point to increase hosting capacity of distributed generation in medium voltage networks, in: 2018 53rd International Universities Power Engineering Conference (UPEC), 2018, pp. 1–6, https://doi.org/10.1109/UPEC.2018.8541861.

[36] L. Zhang, C. Shen, Y. Chen, S. Huang, W. Tang, Coordinated allocation of distributed generation, capacitor banks and soft open points in active distribution networks considering dispatching results, Appl. Energy 231 (2018) 1122–1131, https://doi.org/10.1016/j.apenergy.2018.09.095.

[37] J. Zhao, M. Yao, H. Yu, G. Song, H. Ji, P. Li, Decentralized voltage control strategy of soft open points in active distribution networks based on sensitivity analysis, Electronics 9 (2) (2020) 295, https://doi.org/10.3390/electronics9020295.

[38] P. Cong, Z. Hu, W. Tang, C. Lou, Optimal Allocation of Soft Open Points in Distribution Networks Based on Candidate Location Opitimization, Renewable Power Generation Conference (RPG), Shanghai, China, 2019, pp. 1–6, https://doi.org/10.1049/cp.2019.0270.

[39] P. Cong, Z. Hu, W. Tang, C. Lou, L. Zhang, Optimal allocation of soft open points in active distribution network with high penetration of renewable energy generations, IET Gener., Transm. Distrib. 14 (26) (2020) 6732–6740, https://doi.org/10.1049/iet-gtd.2020.0704.

[40] H. Bastami, M.R. Shakarami, M. Doostizadeh, A decentralized cooperative framework for multi-area active distribution network in presence of inter-area soft open points, Appl. Energy 300 (2021) 117416, https://doi.org/10.1016/j.apenergy.2021.117416.

[41] A. Faramarzi, M. Heidarinejad, B. Stephens, S. Mirjalili, Equilibrium optimizer: a novel optimization algorithm, Knowl. Base Syst. 191 (2020) 105190, https://doi.org/10.1016/j.knosys.2019.105190.

[42] https://globalsolaratlas.info/map.

[43] https://globalwindatlas.info/fr.

[44] A.S. Abbas, A. El-Ela, A. Adel, R.A. El-Sehiemy, Maximization approach of hosting capacity based on uncertain renewable energy resources using network reconfiguration and soft open points, International Transactions on Electrical Energy Systems (2022), https://doi.org/10.1155/2022/2947965, 2022.

[45] T. Dinh Pham, T.T. Nguyen, L.C. Kien, An Improved equilibrium optimizer for optimal placement of distributed generators in distribution systems considering harmonic distortion limits, Complexity (2022), https://doi.org/10.1155/2022/3755754, 2022.

[46] M.A. Shaik, P.L. Mareddy, N. Visali, Enhancement of voltage profile in the distribution system by reconfiguring with DG placement using equilibrium optimizer, Alex. Eng. J. 61 (5) (2022) 4081–4093, https://doi.org/10.1016/j.aej.2021.09.063.

[47] M.Q. Duong, T.T. Nguyen, T.T. Nguyen, Optimal placement of wind power plants in transmission power networks by applying an effectively proposed metaheuristic algorithm, Math. Probl Eng. 2021 (2021) 1–20, https://doi.org/10.1155/2021/1015367.

[48] I. Naruei, F. Keynia, A new optimization method based on COOT bird natural life model, Expert Syst. Appl. 183 (2021) 115352, https://doi.org/10.1016/j.eswa.2021.115352.

[49] M.F. Shaikh, A.M. Shaikh, S.A. Shaikh, R. Nadeem, A.M. Shaikh, A.A. Khokhar, Mitigation of power losses and enhancement in voltage profile by optimal placement of capacitor banks with particle swarm optimization in radial distribution networks, Advances in Electrical and Electronic Engineering 20 (4) (2023) 505–522, https://doi.org/10.15598/aeee.v20i4.4615.

[50] S. Kaur, L.K. Awasthi, A.L. Sangal, G. Dhiman, Tunicate Swarm Algorithm: a new bio-inspired based metaheuristic paradigm for global optimization, Eng. Appl. Artif. Intell. 90 (2020) 103541, https://doi.org/10.1016/j.engappai.2020.103541, 2020.

[51] P.S. Jones, C.C. Davidson, Calculation of power losses for MMC-based VSC HVDC stations, in: 2013 15th European Conference on Power Electronics and Applications (EPE), 2013, pp. 1–10, https://doi.org/10.1109/EPE.2013.6631955.

[52] M.A. Kashem, V. Ganapathy, G.B. Jasmon, M.I. Buhari, A novel method for loss minimization in distribution networks. In DRPT2000. International conference on electric utility deregulation and restructuring and power technologies, No. 00EX382, Proceedings (Cat (2000) 251–256, https://doi.org/10.1109/DRPT.2000.855672. IEEE.

[53] E. Karunarathne, J. Pasupuleti, J. Ekanayake, D. Almeida, The optimal placement and sizing of distributed generation in an active distribution network with several soft open points, Energies 14 (4) (2021) 1084, https://doi.org/10.3390/en14041084.

[54] N.K. Meena, A. Swarnkar, N. Gupta, K.R. Niazi, Multi-objective Taguchi approach for optimal DG integration in distribution systems. IET Generation, Transm. Distrib. 11 (9) (2017) 2418–2428, https://doi.org/10.1049/iet-gtd.2016.2126.

[55] S.K. Sudabattula, M. Kowsalya, Optimal allocation of solar based distributed generators in distribution system using Bat algorithm, Perspectives in Science 8 (2016) 270–272, https://doi.org/10.1016/j.pisc.2016.04.048.

[56] R.S. Rao, K. Ravindra, K. Satish, S.V.L. Narasimham, Power loss minimization in distribution system using network reconfiguration in the presence of distributed generation, IEEE Trans. Power Syst. 28 (1) (2012) 317–325, https://doi.org/10.1109/TPWRS.2012.2197227.

[57] M.Q. Duong, T.D. Pham, T.T. Nguyen, A.T. Doan, H.V. Tran, Determination of optimal location and sizing of solar photovoltaic distribution generation units in radial distribution systems, Energies 12 (1) (2019) 174, https://doi.org/10.3390/en12010174.

[58] L.C. Kien, C.T. Hien, T.T. Nguyen, Optimal reactive power generation for transmission power systems considering discrete values of capacitors and tap changers, Appl. Sci. 11 (12) (2021) 5378, https://doi.org/10.3390/app11125378.

[59] Y. Baghzouz, S. Ertem, Shunt capacitor sizing for radial distribution feeders with distorted substation voltages, IEEE Trans. Power Deliv. 5 (2) (1990) 650–657, https://doi.org/10.1109/61.53067.

[60] T.L. Van, T.H. Nguyen, D.C. Lee, Advanced pitch angle control based on fuzzy logic for variable-speed wind turbine systems, IEEE Trans. Energy Convers. 30 (2) (2015) 578–587, https://doi.org/10.1109/TEC.2014.2379293.

[61] V. Akhmatov, Analysis of Dynamic Behavior of Electric Power Systems with Large Amount of Wind Power. Doctoral Dissertation, Ph. D. Dissertation, Technical University of Denmark, Kgs. Lyngby, Denmark, 2003.
[62] M.K. Behera, I. Majumder, N. Nayak, Solar photovoltaic power forecasting using optimized modified extreme learning machine technique, Engineering Science and Technology, an International Journal 21 (3) (2018) 428–438, https://doi.org/10.1016/j.jestch.2018.04.013.
[63] R.J. Mustafa, M.R. Gomaa, M. Al-Dhaifallah, H. Rezk, Environmental impacts on the performance of solar photovoltaic systems, Sustainability 12 (2) (2020) 608, https://doi.org/10.3390/su12020608.
[64] Y.M. Atwa, E.F. El-Saadany, M.M.A. Salama, R. Seethapathy, Optimal renewable resources mix for distribution system energy loss minimization, IEEE Trans. Power Syst. 25 (1) (2009) 360–370, https://doi.org/10.1109/TPWRS.2009.2030276.
[65] E.S. Oda, A.M. Abd El Hamed, A. Ali, A.A. Elbaset, M. Abd El Sattar, M. Ebeed, Stochastic optimal planning of distribution system considering integrated photovoltaic-based DG and DSTATCOM under uncertainties of loads and solar irradiance, IEEE Access 9 (2021) 26541–26555, https://doi.org/10.1109/access.2021.3058589.